Rock Physics of Reservoir Rocks with Varying Pore Water Saturation and Pore Water Salinity

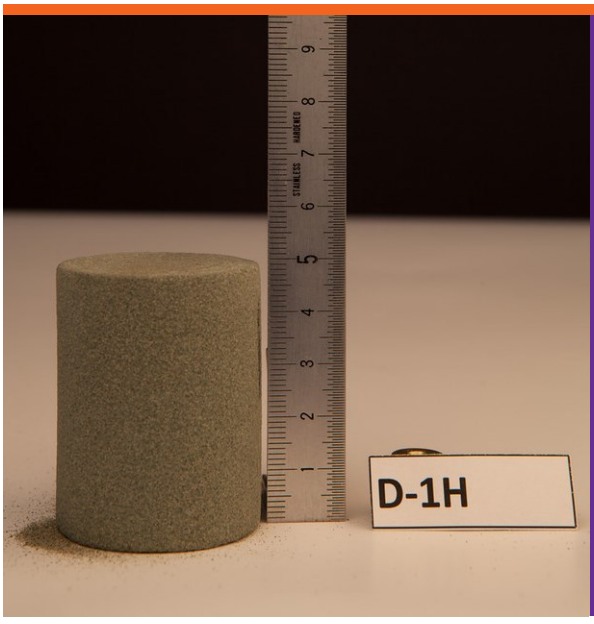

Konstantina Katika

PhD Thesis

Department of Civil Engineering
2016

DTU Civil Engineering Report R-349

DTU Civil Engineering
Department of Civil Engineering

Rock Physics of Reservoir Rocks with Varying Pore Water Saturation and Pore Water Salinity

Konstantina Katika

PhD Thesis
December 2015

DTU-BYG
Department of Civil Engineering
Technical University of Denmark

DTU BYG
Department of Civil Engineering
Technical University of Denmark

Brovej, Building 118
2800 Kongens Lyngby, Denmark
Phone +45 45251700
www.dtu.byg.dk

Preface

This thesis is submitted as partial fulfilment of the requirement for the PhD degree at the Technical University of Denmark (DTU). The work has been carried out at the Department of Civil Engineering from 2012 to 2015 under the supervision of Professor Ida Lykke Fabricius. The project was funded by DTU, Maersk Oil, DONG Energy and the Danish Energy Agency as a part of the Smart Water project. The experimental work for this thesis was carried out at DTU, Colorado School of Mines (CSM) and Geological Survey of Denmark and Greenland (GEUS; co-operation with senior Petrophysicist Dan Olsen). Three months of external research (theoretical and experimental) was performed at the Colorado School of Mines, USA, under the supervision of Professor Manika Prasad at the department of Petroleum Engineering.

This is a paper-based thesis and includes four journal papers (Katika et al., I, II, III and IV). The papers comprise two published paper, one manuscript under review and one manuscript ready for submission (Appendix I). Katika et al., I is discussed in Chapter 7, Katika et al., II in Chapter 8, Katika et al., III in Chapter 9 and Katika et al., IV in Chapter 10 of the thesis. Additional work, conducted during the PhD studies, comprise one submitted journal paper, in collaboration with KU Leuven, along with four conference abstracts (Appendix II).

Unless otherwise indicated, the experimental work in this thesis was performed by the PhD student herself using the lab facilities at DTU, CSM and GEUS. Rock mechanics experiments in Katika et al., II were performed by Mouadh Addassi. The quantification of oil in Katika et al., IV using UV/Visible spectroscopy were performed by Amalia Y. Halim, image analysis by Mehrdad Ahkami, and liquid scintillation analysis by Ioannis Xiarchos. The XRD spectra and BSEM images in Katika et al., I & III were analysed by Ida L. Fabricius.

Summary

Advanced waterflooding (injection of water with selective ions in reservoirs) is a method of enhanced oil recovery (EOR) that has attracted the interest of oil and gas companies that exploit the Danish oil and gas reservoirs. This method has been applied successfully in oil reservoirs and in the Smart Water project performed in a laboratory scale in order to evaluate the EOR processes in selected core plugs. A major step towards this evaluation is to identify the composition of the injected water that leads to increased oil recovery in reservoirs and to define changes in the petrophysical properties of the rock due to the water injection. During advanced waterflooding of reservoirs, or in the Smart Water project, during core flooding experiments, several chemical and petrophysical processes occur in the grains and pore space due to rock, brine and oil interactions. These processes may affect the rate and amount of oil recovered.

Advanced waterflooding experiments of reservoir rocks are performed on laboratory scale, but the mechanisms that describe the effects of water injection on the rock minerals are poorly understood. After many decades, a methodology on how this technique should be performed on specific geological structures and why it is sometimes successful; has yet to be established. The presence of both oil and water in the pore space, several different ions present in the injected water that contact the pore walls, possible changes in the fluid wetting the surface of the grains and high stress applied on the minerals, comprise the complex system of waterflooding. These parameters affect the fluid/fluid, solid/fluid and solid/solid interfaces. The changes of the petrophysical and mechanical properties of the core affected from waterflooding are the main topic of research in the present study. In an effort to simplify the complex system of waterflooding, the parameters that affect the solid/fluid interfaces simultaneously, during the experiments, are studied individually.

Many chemical and petrophysical phenomena have been documented in previous studies that may affect either the mechanical or physical properties of the rock during waterflooding experiments. The phenomena include decreased pore stiffness and subsequent compaction and can be related to a variety of parameters; including precipitation and dissolution reactions, as well as adsorption reactions and changes in

wettability. In order to understand the potential mechanisms under the action of water injection, the present study investigates the effect of the selected ions on the solid/fluid interface of the porous medium under reservoir conditions by studying the following conditions separately: 1) during coreflooding experiments, the rock is subjected to high external stresses that resemble the reservoir stresses; 2) the fluid distribution within the pore space changes during the flow through experiments and wettability alterations may occur; 3) different ions, present in the salt water injected in the core, interact with the surface of the mineral.

This study aims to improve the theoretical understanding of the detailed mechanisms involved in waterflooding, using advanced and sensitive tools on a laboratory scale to illustrate the potential mechanisms behind the action of water injection on oil and brine bearing rocks. In order to investigate the action of pore water with selective ions on the solid/fluid interface, low field nuclear magnetic resonance (NMR) spectrometry, ultrasonic velocities, electrical resistivity and mineralogical characterization are performed on quarry and reservoirs cores. The rocks are saturated with fluids similar to the ones used in the core flooding experiments. Ultrasonic velocities and electrical resistivity data are collected to detect changes with respect to strength and pore geometry of the rock. Low field NMR spectrometry is used to detect changes in texture, wettability and pore-fluid distribution. While investigating the petrophysical properties of reservoir rocks, information concerning the mineralogy is an important factor for the establishment of a rock physical model. Therefore, additional experiments are performed; X-ray diffraction (XRD), backscatter electron microscopy images (BSEM), mercury injection capillary pressure (MICP) curves and specific surface analysis (BET) illustrate the mineralogy and texture of the rock samples.

Chalk from Stevns Klint near Copenhagen, Denmark, (a rock analogue to reservoir chalk from the North Sea) was used for rock mechanical testing in order to understand the potential mechanisms behind the action of ions in high concentration on the chalk surface; such as precipitation and dissolution. The effect of the divalent ions on the elasticity and pore collapse of this rock was observed and validated from the ultrasonic velocity data. Low field NMR was used to detect any precipitation that may occur in the

pore space of chalk saturated with divalent ions. Precipitation occurred only in single cases; therefore, it is doubtful whether it is the responsible mechanism for the water weakening of chalk. The same rock material was used to illustrate the use of low field NMR to detect differences in the texture of chalk; in our case a carbonate mudstone and a carbonate wackestone as previously observed by electron microscopy.

The solid-fluid affinity of chalk from the Gorm field, Berea sandstone and chlorite bearing greensand from the Solsort field was defined from low field NMR data. Longitudinal relaxation time (T_1), transverse relaxation time (T_2) and self-diffusion coefficient of the fluids within the core plugs were measured at different saturation states; water, reservoir oil and oil and water at irreducible water saturation. T_1/T_2 ratio proved a non-destructive and fast way to determine the solid-fluid affinity and fluid distribution within the pore space of the selected rocks.

Finally, supplementary experimental work includes the determination of small amounts of oil in water samples from the NMR T_2 distribution. Low field NMR spectrometry was able to accurately determine the oil and water volume in effluents. This is found very useful, because when the oil reaches residual saturation during core flooding experiments, the produced oil is very small and the quantification of these fluids is often difficult.

Dansk resumé

Der er de senere år blandt danske kulbrinteproducenter opstået interesse for metoder til øget olieudvinding fra reservoirer ved hjælp af injektion af vand med et specifikt indhold af opløste salte. Udenlandske erfaringer viser at injektion af den type vand kan virke, og i øjeblikket er forskere i gang med at undersøge de bagvedliggende mekanismer ved hjælp af laboratorieforsøg på bjergartsprøver. Det vigtigste i denne sammenhæng er at definere den optimale sammensætning af saltene, og at undersøge om reservoirbjergartens fysiske egenskaber ændres som følge af vandinjektionen. Vi må nemlig forvente, at vandinjektionen medfører både fysiske og kemiske ændringer af det porøse medium og porevæsken. Sådanne ændringer kan påvirke udvindingsgraden og udvindingshastigheden af kulbrinterne.

På trods af en omfattende forskningsindsats er mekanismerne bag den øgede kulbrinteudvinding stadig genstand for debat og tydeligvis ikke klart forstået. Det betyder, at selvom denne type vandinjektion gennem flere årtier har vist sig nogen gange at virke, ved man ikke hvorfor. Systemet er også komplekst: Der er både porevand, injektionsvand, kulbrinter og bjergartens mineraler tilstede, derudover har bjergartskornenes kontaktcement og ydre mekaniske belastning, samt reservoirets temperatur og poretryk formentlig betydning, ikke mindst da de indvirker på grænsefladerne mellem: mineralerne, mineral og væske, samt de to væskefaser. I nærværende studium er det vandinjektionens mulige indflydelse på reservoirbjergartens petrofysiske og bjergartsmekaniske egenskaber, der er i fokus. Vi undersøger problemet ved at ændre styrende parametre en ad gangen. Det er således undersøgelsens formål at komme nærmere en teoretisk forståelse af, hvordan vandinjektionen påvirker kontakten mellem mineral og væske.

Vi anvender avancerede og følsomme laboratoriemetoder til at komme nærmere problemets løsning. Mere specifikt er det undersøgelses formål at identificere og kvantificere de processer i porerummet og deraf følgende ændringer, vandinjektionen kan forårsage af de petrofysiske og mekaniske egenskaber af bjergartsprøver fra danske oliefelter og prøver fra stenbrud, der kan tjene som analog til reservoirbjergarter. Tidligere undersøgelser har peget på adskillige kemiske og fysiske ændringer, der vil

kunne påvirke bjergartens petrofysiske eller mekaniske egenskaber under vandinjektion. Det kan dreje sig om mindsket porestivhed og deraf følgende kompaktion, om kemisk udfældning og opløsning, samt om adsorption og desorption på mineraloverfladerne inklusive ændringer i fugtpræference.

For at kunne forstå de potentielle mekanismer bag den øgede olieudvinding, har vi undersøgt effekten af vandinjektion ved reservoirbetingelser, det vil sige ved høj temperatur og høj ydre belastning. Fordelingen af kulbrinter og vand i porerummet ændres som følge af injektionen, og fugtpræferencen kan muligvis ændres. Injektionsvandets saltsammensætning varieres med én jon ad gangen. Nogle joner kan adsorberes på mineraloverfladerne.

For at kunne måle, hvordan tilførslen af specifikke joner påvirker mineraloverfladen bruger vi lavfelts kernemagnetisk resonansspektrometri (NMR), ultralydshastighed, specifik elektrisk modstand og mineralogisk karakterisering. Prøver fra reservoirer og stenbrud mættes med de same væsker som de prøver, der bruges til vandinjektionsforsøg. Ultralydsmålinger og elektriske målinger har til formål at afdække ændringer i porestivhed og poregeometri. NMR vil kunne afdække ændringer i tekstur, i fugtpræference og i fordelingen af olie og vand i porerummet. For at kunne forstå disse ændringer må vi kende mineralogien og den kvantificeres ud fra røntgendiffraktion og elektronmikroskopi. Elektronmikroskopi og kviksølvinjektions data giver sammen med målt specifik overflade et mål for bjergartens tekstur.

Som analog til kalk fra Nordsøen, brugtes prøver af skrivekridt fra Stevns til bjergartsmekaniske forsøg for at afdække hvordan for eksempel opløsning og udfældning styres af porevandets salte. Den kendte blødgørende effekt af divalente joner blev iagttaget, og bekræftet af ultralydsdata, men ved hjælp af NMR blev der kun i enkelte tilfælde påvist udfældninger i porerummet, så det er tvivlsomt om dette er årsagen til de blødere prøver. På de samme kalkprøver kunne der på NMR signalet ses en klar afspejling af bjergartens sedimentære tekstur som iagttaget ved elektronmikroskopi.

For at undersøge NMRs potentiale for at bestemme fugtpræference blev prøver af nordsøkalk, Bereasandsten og chloritdomineret grønsand mættet med porevand, med olie, samt med vand og olie ved irreducibel vandmætning. Her blev både T_1, T_2 og effekten af diffusion, D, målt som funktion af hinanden, og det påvistes, at man som noget nyt, på grund af lokale magnetfelter i mineralerne, kan kvantificere fugtpræferencen ved at sammenligne T_1/T_2 af vand/olieholdige og rent vandholdige prøver. Dette resultat har potentiale i forbindelse med tolkning af fugtpræference ud fra petrofysiske NMR logs.

Til kvantificering af små oliemængder i vandprøver viste NMR sig uhyre præcis omend noget tidskrævende. Dette er specielt relevant ved vandinjektionsforsøg, hvor de ekstra producerede oliemængder kan være små i forhold til det producerede vand.

Acknowledgements

First of all I would like to express my deep appreciation to my main supervisor, Professor Ida Lykke Fabricius. She trusted me for being one of her students and taught me the virtues of patience and hard work. She provided support and advice during this project and allowed me the freedom to pursue my own ideas and interests. Our cooperation enhanced my knowledge in geology and chemistry and many other aspects of science and made me the researcher I am today. My sincere gratitude also goes to my co-supervisor of the first two years, M. Monzurul Alam, for his assistance, guidance, technical and moral support. His door was always open for me and he succeeded in passing his passion for experiments and hard work to me.

I acknowledge the Danish Energy Agency, Mærsk Oil and DONG Energy for funding the research and providing the core data. I am thankful to Alexander Shapiro, Ioannis Xiarchos and all members of the SmartWater project for valuable discussions, suggestions and technical assistance. Special thanks to Dan Olsen and Hans Jørgen Lorentzen of Geological Survey of Greenland and Denmark (GEUS) for helping with saturating the samples and to Henrik Fordsmand for helping me with the NMR equipment in the facilities of Haldor Topsoe.

I thank Professor Manika Prasad of Colorado School of Mines for accepting me for my external study and for her kind assistance and advice during my stay in Golden. I also thank Milad Saidian for his support and advice during my external stay. I especially thank Varvara Zania for the great time and scientific discussions we had inside and outside the working environment the past three years. I feel lucky to get very good colleagues during these years; our office in the long corridor of 119 was always a friendly, creative and productive work environment. Special thanks to Chiara Latini and Lisa Pasquinelli. Thanks also to my fellow lab colleagues, especially Morten Kanne Sorensen and Tobias Orlander. Experimental work is often associated with frustration, and it has been nice to share this with good friends in the office and the lab. A huge thank to Sinh Nguyen and Hector Diaz of DTU-Environment and Tran Thuong Dang, Zacarias Tecle and Duc Thuong Vu of DTU-Chemical Engineering for assisting

laboratory work and to John Troelsen for being always helpful and cheerful. Katrine Alling Andreassen, Amalia Yunita Halim and all the master students I had the pleasure to work together with in the lab are also acknowledged. I would like to thank my colleague and friend Artem Alexeev for all the fruitful and challenging scientific discussions we had. We started our PhD studies together and he was always supportive and understanding.

I couldn't thank enough my friends here in Copenhagen; they taught me how to survive both in DTU and in Denmark. Katerina, Carolina, Elena, Anthi, Eirini, Eirini, Meleti, Thalia and Filippo your presence during these years made me feel like I never left home. I am also thankful to Darlene and Will who provided a home for me in Golden. I would like to express my gratitude to the people who supported my first steps and make me feel like they never left my side, even though we don't live in the same place anymore; Babi, Fotini, Katerina, Kostanti, Maria, Mariangela, Marko, Taso and Vasia, you are gratefully acknowledged.

I would like to thank my mom and dad who despite everything happening in their life, provided a safe and relaxed atmosphere for me to work so far away from them. They always support my decisions and make me feel that they have my back. They are always comforting about my troubles and proud of my achievements. The rest of my big lovely family is also acknowledged. Afroditi, Antoni and Thodori thank you for making me smile all the way from London.

Konstantina Katika
November 2015
Kgs. Lyngby, Denmark

Dedicated to my sister

List of publications

Thesis contributions

Katika et al., I: Katika, K., Addassi, M., Alam, M.M., & Fabricius, I.L., 2014, Changes in Specific Surface as observed by NMR, caused by saturation of Chalk with porewater bearing divalent Ions, *Diffusion Fundamentals*, **22**, 1–14.

Katika et al., II: Katika, K., Addassi, M., Alam, M.M., & Fabricius, I.L., 2015, The effect of divalent ions on the elasticity and pore collapse of chalk evaluated from compressional wave velocity and low-field NMR, *Petroleum Science and Engineering*, **136**, 88–99.

Katika et al., III: Katika, K., Saidian, M., Prasad, M., & Fabricius, I.L., Low field NMR spectrometry of chalk and argillaceous sandstones: rock - fluid affinity assessed from T_1/T_2 ratio, to be submitted to the journal of *Petrophysics*.

Katika et al., IV: Katika, K., Ahkami, M., Fabricius, I.L., Fosbøl, P.L., Halim, A.Y., Shapiro, A., Thomsen, K., & Xiarchos, I., Comparative analysis of experimental methods for quantification of small amounts of oil in water, under review, journal of *Petroleum Science and Engineering*.

Additional contributions

Fay-Gomord, O., Soete, J., Katika, K., Galaup, S., Caline, B., Descamps, F., Lasseur, E., Fabricius, I.L., Saiag, J., Swennen, R., & Vandycke, S., New Insight into the Microtexture of Chalks from NMR Analysis, submitted to the journal of *Marine and Petroleum Geology*.

Katika, K., Alam, M.M., & Fabricius, I.L., 2013, Nuclear magnetic resonance and sound velocity measurements of chalk saturated with magnesium rich brine, *Poromechanics V* (ISBN: 978-0-7844-1299-2), 678-684, ASCE.

Katika, K., Alam, M.M., & Fabricius, I.L., 2013, Nuclear Magnetic Resonance and Elastic Wave Velocity of Chalk Saturated with Brines Containing Divalent Ions, presented at: 75th EAGE Conference & Exhibition incorporating, London, UK.

Alam, M.M., Katika, K., & Fabricius, I. L., 2014, Effect of salinity and specific ions on amount of bound water on quartz, calcite and kaolinite, as observed by NMR transverse relaxation time (T_2), presented at: 76th EAGE Conference & Exhibition, Amsterdam, The Netherlands.

Katika, K., & Fabricius, I. L., 2015, Electrical tortuosity, Kozeny's factor and cementation factor modelled for chalk, presented at: 3rd international Workshop on Rock Physics, April 2015, Perth, Australia.

Table of contents

1 Introduction

1.1 Research objectives

Advanced waterflooding has attracted the interest of the industry that exploits the Danish oil and gas reservoirs in the North Sea. Two different reservoir rocks are of primary interest; chalk and greensand. In the present study, chalk of Tor Formation is from the Gorm field and chlorite-bearing greensand is from the Solsort field. Chalk from Stevns Klint and Berea sandstone are also used. These rocks are often used as rock analogues due to the similar petrophysical properties to reservoir rocks, high availability and low cost. The PhD thesis is a part of a large collaborative project (Smart Water) between oil industry and university. The aim of the project is to improve the theoretical understanding of the detailed mechanisms involved in water flooding and formulate proposals for pilot water flooding in Danish oil and gas reservoirs in the North Sea.

The overall scientific goal of this thesis is to identify and quantify the physical processes on a pore scale that are responsible for changes in petrophysical and mechanical properties of reservoir and quarry rocks caused by pore water with selective ions and salinity. This study was performed to understand some of the challenges related to advanced waterflooding applications in the Danish reservoirs in the North Sea (chalk and greensand reservoirs) and phenomena related to water injection with selected ions. Low field Nuclear Magnetic Resonance (NMR) and ultrasonic velocities comprise the main tools of the research on reservoir and quarry rocks. The main research objectives are listed below:

1. The first objective is to use low field nuclear magnetic resonance (NMR) spectrometry in order to study how selected ions used for water injection alter the specific surface of the grains of chalk and as a result, the physical and chemical environment of the pore space. Fines migration, dissolution, precipitation reactions, wettability alterations and other related phenomena alter the surface of the grains, and may be attributed to the presence of selected ions in the pore space of the rock.

2. The second objective is to study whether the selected ions used for water injection affect the elasticity and pore collapse of chalk. The chemical composition of the fluid, used for saturation and flooding, affects the mechanical strength of the chalk and has been related to a variety of parameters; including precipitation and dissolution reactions, as well as adsorption reactions and changes in wettability.

3. The third objective is to define the solid/fluid affinity (wettability) of the reservoir rocks before the water injection and flooding with the use of low field NMR spectrometry. The wettability of reservoir rocks affects the distribution of oil and water and the residual saturations of reservoir fluids. It also influences the amount of oil that is ultimately recoverable as well as the rate at which the oil is recovered. A fast, economical, non-destructive and non-invasive way to determine the wettability of reservoirs is investigated using two dimensional NMR relaxation correlations.

4. The fourth objective is to investigate a suitable technique to determine small amounts of fluids as they are produced during the coreflooding experiments. These fluids are used to validate the enhanced/improved oil recovery processes that occur during water injection experiments in the laboratory. The use of low field NMR to determine small amounts of oil and water in high accuracy is the main contribution of the study.

1.2 Scope of study

This study has been divided into four parts in order to address the main research objectives separately: 1) the first research objective is described in Chapter 7 (Katika et al., I), 2) the second research objective is described in Chapter 8 (Katika et al., II), 3) the third research objective is described in Chapter 9 (Katika et al., III), and 4) the fourth research objective is described in Chapter 10 (Katika et al., IV). The work presented in this thesis is organized into eleven chapters, where the chapters are mainly based on articles that are either published or submitted. A summary of each chapter is given below:

Chapter 1 provides a short introduction to the thesis describing the research objectives and scope of the study.

Chapter 2 reviews published studies of advanced waterflooding for oil recovery. Phenomena related to salt water injection in several reservoir rocks are described; such as, chemical and mechanical changes in the pore space of chalk and the solid-fluid affinity of reservoir rocks.

Chapter 3 reviews published studies of low field NMR spectrometry in porous media. More specifically this chapter discusses the application of low field NMR to define changes in the chemical and mechanical properties of the rock, and for determining the solid-fluid affinity and quantifying small amounts of oil in water.

Chapter 4 provides a description of all the rock material and brines used in the present study; reservoir chalk from the North Sea, chalk from Stevns Klint in Denmark, sandstone from Berea in USA and reservoir greensand from the North Sea. Crude oil from the South Arne field in the North Sea and several synthetic brines are used to saturate the core samples.

Chapter 5 provides a description of all the methods used in this study for petrophysical and rock mechanical investigation and mineralogical determination of the selected material and core plugs.

Chapter 6 summarizes the results from petrography and petrophysical measurements.

Chapter 7 is based on the paper "*Changes in Specific Surface as observed by NMR, caused by saturation of Chalk with porewater bearing divalent Ions*". The way pore water rich in divalent ions affects the transverse relaxation of chalk with two different depositional textures is investigated. The T_2 distribution reflects the pore size distribution and therefore, changes in the specific surface of the pore space can be detected. Two cases are compared. The first experiments on chalk from Stevns Klint

with high salinity brines showed that saturation with divalent ions (Mg^{2+},$Ca^{2+}$and SO_4^{2-}) cause major shifts in the T_2 distribution curve, probably due to the presence of fines in the pore space. In a second set of experiments, fluid samples where precipitation takes place were found to show shifts in the T_2 spectrum due to the creation of crystals. Differences in the rock texture and precipitants within the pore space, which affect the T_2 by altering the surface-to-volume ratio of the pore space, were identified.

Chapter 8 is based on the paper "*The effect of divalent ions on the elasticity and pore collapse of chalk evaluated from compressional wave velocity and low-field NMR*". The effects of divalent ions on the elasticity and the pore collapse of chalk are studied through rock-mechanical testing and low-field NMR spectrometry. Chalk samples saturated with deionized water and brines containing sodium, magnesium, calcium and sulfate ions are subjected to petrophysical experiments, rock mechanical testing and low-field NMR spectrometry. Petrophysical characterization involving ultrasonic elastic wave velocities, porosity and permeability measurements, specific surface and carbonate content determination and backscatter electron microscopy of the materials were conducted prior to the experiments. Low-field NMR spectrometry is used in addition to the mechanical testing to identify changes observed after the saturation related to the surface-to-volume ratio of the pore space in each of the samples. The experimental results reveal that both elasticity and pore collapse are influenced by the presence of divalent ions in distinct ways. Compressional wave velocities indicate that saturation with water rich in magnesium and calcium ions softens the contact among the mineral grains, whereas the presence of calcium and sulfate ions in the saturating fluid results in pore collapse at lower stresses than in the case when samples are saturated with deionized water or sodium chloride solution. Low field NMR spectrometry revealed precipitation of crystals in the pore space of chalk saturated with Mg-rich brine. The precipitation of Mg-carbonates was not used to explain the deteriorating pore collapse strength and effects on the elasticity after the saturation since none of the other plugs saturated with divalent ions (Ca^{2+} and SO_4^{2+}) experienced it.

Chapter 9 is based on the paper "*Low field NMR spectrometry of chalk and argillaceous sandstones: rock - fluid affinity assessed from T_1/T_2 ratio*". The low field nuclear

magnetic resonance (NMR) procedure typically minimises the effects of macroscopic magnetic field gradients on the transverse relaxation. Thus, longitudinal, T_1, and transverse, T_2, relaxation times should in principle be similar. However, microscopic magnetic gradients related to minerals can shorten T_2 relaxation times as compared to T_1 relaxation times provided the saturating fluid has high affinity to the solid. We consequently find that the T_1/T_2 ratio can quantify the affinity between the rock and wetting pore fluid. The affinity is a measure directly linked to wettability. In order to investigate the T_2-shortening, we performed 1D and 2D NMR experiments on different samples of chalk, Berea sandstone, and chloritic greensand, saturated either with water, oil or oil/water at irreducible water saturation. T_2 spectra show that in all water saturated samples, surface relaxation dominates; in oil saturated chalk and Berea sandstone, bulk relaxation dominates; whereas T_2 of oil saturated greensand shows surface relaxation in part of the spectrum. In all three samples with two fluids, water shows surface relaxation and oil shows bulk relaxation. The T_1/T_2 ratio obtained from T_1-T_2 maps reflects the T_2 shortening, so we compare the T_1/T_2 ratio for the same type of rock, saturated with different fluids. The chalk shows high affinity for water, Berea sandstone has no clear preference for oil and water whereas chloritic greensand shows different behaviour for small and large pores as defined in the MICP throat size distribution. Small pores (fast relaxing components) have (T_1/T_2=2.0) when water saturated, but (T_1/T_2=3.8) when oil saturated indicating oil-affinity. By contrast large pores (slow relaxing components) have significant preference for water (T_1/T_2 = 2.2) as compared to oil (T_1/T_2=1.2-1.4). D-T_2 maps of water saturated rocks show effects of macroscopic field gradients, whereas samples saturated with oil or with both oil and water only show macroscopic field gradient effects in the oil phase. This shows that in the last case, the water is trapped between solid and oil and macroscopic field gradients only have minor effects in the water phase. Based on the NMR wettability studies, the fluid distribution in the pore space was determined and applied in Gassmann's fluid substitution.

Chapter 10 is based on the paper "*Comparative analysis of experimental methods for quantification of small amounts of oil in water*". During core flooding experiments, water is injected into oil bearing core plugs and the produced fluids can be sampled in a fraction collector. When the core approaches residual oil saturation, the produced

amount of oil is typically small (can be less than a few microliters) and the quantification of oil is then difficult. In this study, we compare four approaches to determine the volume of the collected oil fraction in core flooding effluents. The four methods are: Image analysis, UV/visible spectroscopy, liquid scintillation counting, and low-field NMR spectrometry. The NMR method is capable of direct quantification of both oil and water fractions, without comparison to a pre-made standard curve. Image analysis, UV/visible spectroscopy, and liquid scintillation counting quantify only the oil fraction by comparing with a pre-made standard curve. The image analysis technique is reliable when more than 0.1 ml oil is present, whereas liquid scintillation counting performs well when less than 0.6 ml oil is present.

Chapter 11 summarizes the main findings and conclusions from this study.

2 Advanced waterflooding for oil recovery

One of the ongoing challenges of the research in oil and gas reservoirs is to enhance oil recovery by altering the salinity and the relative concentration of the ions in the water used in advanced waterflooding. During advanced waterflooding, water with selected ions is injected in the reservoirs and extra oil is produced. Waterflooding is widely used as a method for recovering oil from reservoirs due to a variety of reasons; water can displace efficiently oil of light to medium gravity; water is relatively easy to inject into the rock formations; water is widely available and inexpensive (Yousef et al., 2011). Injecting water of specific ionic composition and salinity is an environmentally friendly technique that requires no additional chemicals to be induced in the formation such as the surfactant flooding which requires the injection of one or more liquid chemicals and surfactants (Hirasaki et al., 2011). Produced water, saline waters from nearby aquifers that are not related to oil-fields and seawater are the most common options for water injection operations, particularly in offshore and near coastal operations (Bader et al., 2006).

Previous studies have validated the success of advanced waterflooding to enhance the oil recovery both from chalk and sandstone reservoirs. Experiments have been conducted in the laboratory, but field testings have also been reported. Low salinity flooding has been successfully used in sandstone reservoirs (Seccombe et al. 2008; Vledder et al., 2010) and effects of changing the composition of the injecting water have been observed in limestones (Morrow et al., 1998; Strand et al., 2006; Austad et. al., 2007).

It is therefore documented, that the composition of injected water can affect the crude oil/brine/rock interactions in a favourable way to improve oil recovery in several reservoir rocks. As the application of waterflooding methods becomes a necessity for additional oil recovery; the research focuses on the impact of water injection on the mechanical and physical properties of the rock. Several observations have been reported that the injection of water may result in changes in the solid-fluid interface and the rock stiffness. Precipitation, fines formation or migration and dissolution reactions, as well as

adsorption reactions and changes in wettability that might influence the solid/fluid interface have been advocated (Fathi et al., 2010; Madland et al., 2011; Ali et al., 2011). Furthermore, the strength of the rock is related to the fluid used for saturation and the injection of water may result in weakening of the rock (Risnes at al., 2003, Andreassen et al., 2010, Megawati et al., 2012).

Three mechanisms related to the above-mentioned observations, and main research objectives of the present study, are: 1) the generation of fines and precipitation or other substitution/adsorption phenomena on the pore wall of the chalk due to the injection of water with various ions (eg. Madland et al., 2011); 2) the changes in the elastic properties of chalk due to solid/fluid interactions (eg. Nermoen et al., 2015); 3) the preference of the chalk and sandstone minerals to either water or oil, that influences the rate and amount of recoverable oil (eg. Morrow et al., 1998).

2.1 Chemical changes on the pore walls of chalk

Related to the first research objective of this study, studies have indicated that the ionic composition of the water present in the pore space may result in precipitation or other substitution/adsorption phenomena on the surface of chalk. Hiorth et al., (2010), investigated how the water chemistry could change the charge on the chalk surface and dissolve minerals and possibly affect the chalk wettability and therefore, the oil recovery. In rocks similar to the Stevns Klint chalk, a chemical model that couples bulk aqueous and surface chemistry and also addresses mineral precipitation and dissolution was constructed and applied. The results indicate that the precipitation/dissolution mechanism can be the controlling factor that influences the oil recovery of carbonate rocks as appeared in laboratory experiments in previous studies (Zhang et al. 2007; Austad et al. 2008).

2.2 Mechanical changes in chalk

Related to the second research objective of this study, authors have illustrated that the mechanical properties of chalk are coupled to the fluid present in the pore space of chalk (e.g. Andreassen et al., 2010). The mechanical properties of chalk are related to

the porosity, the stiffness properties of the grains and how well the grains contact each other. Changes in these properties may be induced due to injection. The water injection has also been associated with compaction; an important drive mechanism for oil recovery from porous chalk reservoirs (Austad et. al., 2008). Simulation studies for the high porosity chalk reservoirs at the Valhall field have indicated that half of the oil production is due to the rock compaction recovery mechanism (Cook and Jewell, 1996). However, rock compaction causes severe environmental problems such as surface subsidence, and seafloor deformation, leading to sinking of offshore platforms, buckled seabed pipelines, and operational problems (Settari, 2002). It is therefore necessary to understand the mechanisms behind the compacting reservoirs, in order to take advantage of the oil recovery mechanisms while minimizing the problems it creates. According to Risnes et al., (2005), strong interaction between the highly polar water molecules and the chalk surface may develop repulsive forces when two surfaces are in close contact and therefore weaken the chalk. Delage et al., (1996) proposed that capillary changes occur between water and oil within the chalk.

A suggested theory regarding water weakening of chalk is the substitution process taking place inside the chalk when seawater-like brines are injected at high temperatures (Korsnes et al., 2006). According to the proposed mechanism, Mg^{2+} in the aqueous phase substitutes Ca^{2+} at intergranular contacts, in the presence of SO_4^{2-}. On the other hand, experiments on Stevns and Leige chalk by Madland et al., (2011), demonstrated that sulphate is not needed to have a significant amount of deformation. Water analysis of the produced fluids was performed and the magnesium ions were found less in the produced than the injected pore water. Two mechanisms were proposed; substitution of calcium and magnesium without the presence of sulfates in the porewater and the precipitation of magnesium as part of a new mineral phase (Madland et al., 2011; Andersen et al., 2012). The increase in Ca^{2+} and decrease in Mg^{2+} concentration in chalk has been attributed to precipitation of $CaSO_4$ in the formation at high temperatures (Puntervold and Austad, 2007).

Nermoen et al., (2015), observed the effect of various brines and oil on the elastic properties of Liege chalk from Belgium, as derived from mechanical testing. The

proposed mechanism is that chalk saturated with brines, which cause high electrostatic potential on the surface of chalk, are the weakest. Nermoen et al., (2015), introduced the repulsive electrostatic stresses as a mechanism that separates the grains of chalk and therefore weakening the saturated sample (Figure 2.1). The authors introduced the electrostatic stress in the effective stress relationship, as a mechanism that decreases the effective stresses in chalk under the presence of certain fluids and ions.

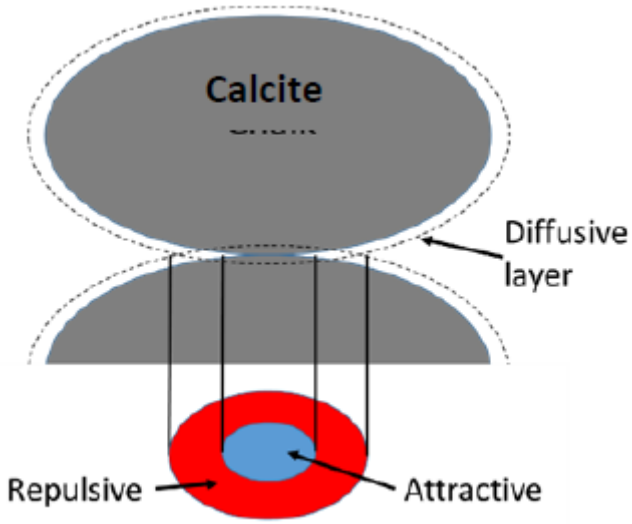

Figure 2.1. Attractive and repulsive forces projected onto the blue and red surface according to Nermoen et al., (2015). Different brines (fluids) display different electrostatic forces.

2.3 Solid-fluid affinity of reservoir rocks

Related to the third research objective of this study, researchers have illustrated the strong connection of wettability to oil recovery. The wettability describes the solid-fluid affinity of a unique system of brine, oil and rock under certain conditions; such as, temperature, pressure and oil and brine properties (Radke et al., 1992). The wettability of reservoir rocks affects the distribution of oil and water and the residual saturations of reservoir fluids (Borgia et. al., 1991). It also influences the amount of oil that is ultimately recoverable as well as the rate at which the oil is recovered (Hsu et al, 1992).

Many studies take into account the initial wettability state of the rock before the water injection and wettability alterations that may occur during the injection. A systematic laboratory study by Jadhunandan and Morrow (1995), on Berea sandstone showed an

optimum in oil recovery by water flooding when the rock is water wet. Hiort et al., (2010), modelled how the injection of water into Stevns Klint chalk could cause mineral dissolution, and this could affect the wettability (Figure 2.2). Several authors working on chalk attributed the effect of injecting water to wettability alterations (Austad et al., 2005; Strand et al., 2006; Zhang et al., 2007; Austad et al., 2008; Yousef et al., 2010). This effect was attributed to the reactivity of key seawater ions (SO_4^{2-}, Ca^{2+}, Mg^{2+}) that have the capability to change the rock surface charges.

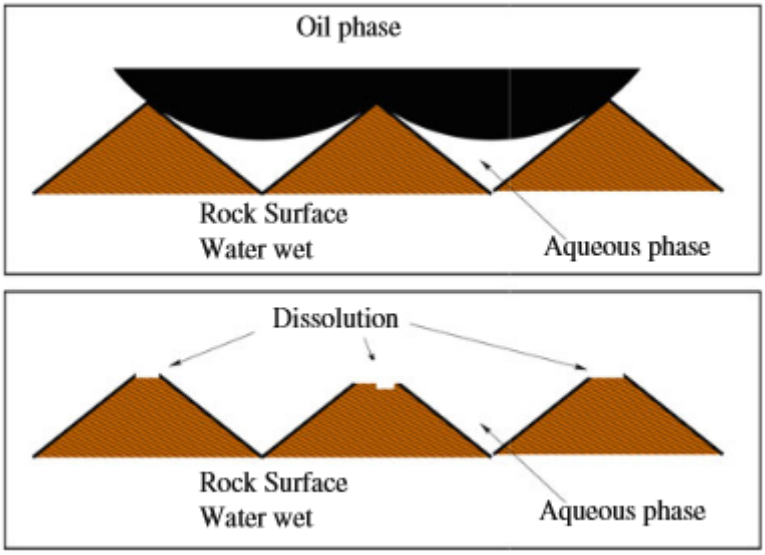

Figure 2.2. Changes in the wettability of chalk due to dissolution according to Hiorth et al., (2010). Top: A section of the pore space, before any dissolution reaction. The surface is rough and oil is attached where there is a large curvature and the water film is broken. Bottom: Dissolution of the chalk surface has taken place where the oil was attached, and new rock surface has been created.

3 Low field NMR spectrometry

Low field Nuclear Magnetic Resonance (NMR) spectrometry is based on the fact that nuclei of hydrogen atoms have magnetic properties that can be utilized to yield chemical and physical information on the environment of these nuclei (Dunn et al., 2002). The nuclear spin of hydrogens in a fluid can be aligned in a temporary magnetic field and then relax. The signal of the relaxation rate is proportional to the population of hydrogen atoms in the sample, and the viscosity of the fluid. Therefore, it is natural to consider using these NMR properties for oil exploration (Dunn et al., 2002). Low field NMR spectrometry in porous media is based on the increase in relaxation rate of hydrogen nuclei in fluids when confined in the pores compared to the bulk response (Kleinberg et al., 1994). Also, it is based on the variation of relaxation rates when different fluids (e.g. oil or water) contact surfaces with different solid fluid affinities (Borgia et al., 1991). Several parameters measured from NMR spectrometry, including, T_2, (transverse relaxation time), T_1 (longitudinal relaxation time) and the self-diffusion coefficient of the fluid within the samples, D, can provide information concerning the petrophysical properties of the porous medium; such as the viscosity of the saturating fluid (Hirasaki et. al., 2003), the pore geometry and saturation (Hürlimann et al, 2002).

3.1 Low field NMR spectrometry in porous media

The NMR procedure starts as an absorption process, where hydrogen nuclei are brought to align their spin, and the nuclei in the excited state must be able to return to the ground state (relax). Low field NMR spectrometry is performed at low Larmor frequencies (Kleinberg et al., 1994). Energy is absorbed and emitted from the hydrogen nuclei when they resonate to this frequency and therefore, relax. There are two processes that restore relaxation in NMR spectrometry: longitudinal (spin-lattice) relaxation and transverse (spin-spin) relaxation (Dunn et al., 2002).

Longitudinal relaxation is the result of driving the longitudinal magnetization of the hydrogen nuclei to the equilibrium position, which is, aligned with an external magnetic field. In longitudinal relaxation, energy is transferred to the molecular framework

(lattice). This type of energy is lost as vibrational or translational energy. The characteristic time constant related to the longitudinal relaxation is called longitudinal, or spin-lattice relaxation time, T_1, and is described from the following equation (Dunn et al., 2002):

$$M(t) = M_0(1 - 2e^{-t/T_1}). \quad (3.1)$$

The magnetization of the system, *M*, gradually builds up until it reaches the equilibrium value, M_0, which is the net magnetization of the system.

The thermal motions of the lattice are the motivating force to stimulate the transitions between the magnetic energy levels by emitting or absorbing energy to or from the surroundings of the nucleus. This kind of process, called transverse or spin-spin relaxation, eventually leads to thermal equilibrium. The characteristic time constant related to the transverse relaxation is called transverse, or spin-spin relaxation time, T_2, and is described from the loss of magnetization of the system, *M* (Dunn et al., 2002):

$$M(t) = M_0 e^{-t/T_2}. \quad (3.2)$$

Longitudinal and transverse relaxations may both be affected by the bulk relaxation of the fluid; when the interface of the fluid with the solid is minimized. They are also affected by the surface relaxation due to the solid-fluid interaction (Kleinberg et al., 1994). In principle, the bulk and surface relaxation are similar for both longitudinal and transverse relaxation; because the molecular mobility causing the nuclei to relax is the same (Dunn et al., 2002). A third mechanism, that affects the transverse more than the longitudinal relaxation, is the effect of macroscopic and microscopic field gradients which promote faster relaxation. The Inversion Recovery Free Induction Decay pulse sequence (IRFid) has the advantage of measuring the longitudinal relaxation and almost eliminating any effects due to microscopic and macroscopic field gradients (Dunn et al., 2002). Macroscopic field gradients can be neglected when transverse relaxation measurements are performed with the use of CPMG pulse sequence at low Larmor frequencies (Kleinberg et al., 1994). The CPMG pulse sequence was named after the pairs of authors: Carr, Purcell, Meiboom and Gill (cited in Dunn et al., 2002). This procedure does not eliminate effects of microscopic field gradients in transverse relaxation. These may be caused by a variety of reasons; such as the presence of

paramagnetic minerals and a magnetic susceptibility difference between the fluid and the surface of the mineral (Dunn et al., 2002). The microscopic field gradients only affect fluids wetting the mineral surface. When molecules adsorb on surfaces, changes in their translational and rotational dynamics accelerate the transverse relaxation resulting in $T_1 > T_2$ (McDonald et al., 2005). They are difficult to predict precisely, so such effects are measured experimentally (Sun and Dunn, 2002).

The loss of transverse magnetization due to field gradients of the system becomes (Dunn et al., 2002):

$$M(t) = M_0 e^{-t\left(\frac{1}{T_2}+(\gamma \nabla H)^2 D\frac{\tau^2}{3}\right)} \quad (3.3)$$

where, $1/T_2$ is the decay rate of transverse magnetization in a uniform fluid, τ is the time interval used in the dephasing and rephasing periods of the spin echo experiments in the CPMG pulse sequence, D is the self-diffusion coefficient of the atom possessing the nuclear spin in the fluid, γ is the nuclear gyromagnetic ratio, and ∇H is the field gradient. In known induced macroscopic field gradients, g, (i.e. during NMR self-diffusion coefficient measurements), the self-diffusion coefficient of a fluid may be determined form equation (3.3).

After each NMR measurement, an inversion technique converts the longitudinal and transverse relaxation decay curve into a T_1 and T_2 spectrum respectively. Assuming that the bulk fluid relaxation is slow compared to surface relaxation, and that the relaxation due to diffusion is negligible; the longitudinal relaxation rate, $1/T_1$ (1/s), is proportional to the surface-to-volume ratio, S/V (1/μm) or the specific surface of the pore space, S_ϕ (1/μm), and the surface relaxivity, ρ_1 (μm/s) (Coates et. al., 1999):

$$\frac{1}{T_1} = \rho_1 \frac{S_p}{V} \quad or \quad \frac{1}{T_1} = \rho_1 S_\phi. \quad (3.4)$$

Similarly, the transverse relaxation rate is related to the surface relaxivity, ρ_2 (μm/s) and given by the following equation (Coates et. al., 1999):

$$\frac{1}{T_2} = \rho_2 \frac{S_p}{V} \quad or \quad \frac{1}{T_2} = \rho_2 S_\phi. \quad (3.5)$$

The surface relaxivity, $\rho_{1,2}$, is a constant that connects the surface-to-volume ratio (S/V) to the relaxation rate and quantifies the ability of a mineral to enhance relaxation (Keating and Knight, 2012). The surface relaxation is related to the interaction of the fluid molecules with the pore wall, and thus with their average distance from the wall. Therefore, the distribution of $T_{1,2}$ reflects the pore size distribution of the rock.

3.2 Low field NMR spectrometry in advanced waterflooding

Low field NMR spectrometry can be utilised to define the mechanisms that govern the enhanced oil recovery mechanisms in advanced waterflooding. NMR spectrometry is sensitive to changes in the solid/fluid interface, hence it can be a helpful tool to assist in the answer of the main research objectives that are reported in the present study; 1) changes in the specific surface of the pore space of a rock due to precipitation or dissolution/adsorption and other chemical phenomena which 2) are often related to decreased pore stiffness and compaction; 3) the preference of a mineral to a certain fluid (in many studies described as wettability) and the pore fluid distribution. In addition, 4) low field NMR spectrometry can directly measure the density of hydrogen nuclei in reservoir fluids and determine the presence and quantities of the different fluids (water, oil, and gas) (Coates, 1999). Therefore, low field NMR spectrometry can be applied to quantify small amounts of oil and water in effluents from flooding experiments.

3.2.1 The use of NMR to define mineralogical changes

Related to the first and second research objective of the present study, Yousef et al., (2011), performed NMR measurements on cores subjected to water injection in advanced waterflooding experiments in the laboratory. Diluted seawater injection caused a significant enhancement in the surface relaxation of the carbonate rock and a change of shape in the T_2 distribution. The enhancement of the surface relaxation and changes in the shape of the T_2 distribution were attributed to the rock dissolution.

Megawati et al., (2012), obtained the NMR relaxation of chalk from Stevns Klint, Liege and Kansas loaded in elastic region (before yield) and in plastic region (after yield).

Experiments on fully water saturated cores illustrated that the $T_{1,2}$ distributions were shifted, reflecting pore size reduction following volumetric strain.

Grombacher et al., (2012), performed NMR experiments on carbonate rocks in order to determine how chemical alteration and dissolution affect the T_2 distribution. In several carbonates, shifting peaks of the T_2 were explained by dissolution creating a rougher pore surface, leading to a higher surface-to-volume ratio (and T_2). In other carbonate rocks only minor changes in the T_2 were found after the water injection. All observations were supported by BSEM images, CT scans and changes in the elastic waves. The dissolution resulted in softening of the carbonate rock due to changes of the grain-contact stiffness that did not alter the specific surface of the pore space.

Diaz et al., (1999), used low field NMR spectrometry to study the presence of tiny suspended particles in the pore fluid that alter the surface relaxation. A major drawback in waterflooding of Mina el Carmen reservoirs in Argentina was the invasion of solids, which caused formation damage and, consequently, inhibited injection and ceased production. Based on the NMR log and core data, they were able to establish the correlation between the T_2 distributions in the formation and the threshold solid particle size allowed in the injection water, which was important to prevent formation damage.

3.2.2 The use of NMR to define wettability and fluid distribution

Related to the third research objective of the present study, NMR spectrometry may be used for wettability assessment of oil and gas reservoirs. Based on the wettability, the pore fluid distribution of the rock can be determined. The fluid distribution is an important parameter in assessing the elasticity of oil and water saturated porous rocks. In a log interpretation context, elasticity data can be corrected by Gassmann's (1951) fluid substitution if the fluid distribution of the pore space is known.

3.2.2.1 NMR log analysis

Freedman et al., (2003), performed laboratory experiments on Berea sandstones using NMR tools intended for log analysis. The crude oil T_2 distributions for partially

saturated rocks were compared with the T_2 distribution of the bulk oil and illustrated the water wetness of the rock. In laboratory conditions, the noise and other parameters, which interfere with the log measurements, are eliminated, but the most widely used NMR logging tools measure T_1 and T_2 in the presence of internal field inhomogeneities (Heaton et al., 2002). Additionally, NMR logging is an expensive procedure, and lengthy and time consuming measurements of high accuracy, cannot be obtained. Therefore, the need to compare NMR logging data with NMR data of high accuracy obtained in the laboratory is required for the accurate estimation of NMR wettability.

3.2.2.2 T_1 and T_2 distributions

In laboratory conditions, NMR core analysis can be a non-destructive and accurate tool to determine the wettability. Hsu et al., (1992) compared T_1 measurements to the combined Amott/USBM method to determine successfully the wettability of carbonate core plugs. Guan et al., (2002) and Al-Mahrooqi et al., (2002) obtained the same conclusions by studying saturated outcrop sandstones and comparing NMR results to the Amott–Harvey (AH) index.

In the above-mentioned studies, T_1 and T_2 are used to describe the preference of a solid to a certain fluid. In most case studies, the rocks are saturated with a single fluid; either water or oil, but in real reservoirs, the rock is usually saturated with both oil and water. Therefore, it is necessary to map the wettability of a rock in a state when both oil and water are able to wet the surface of the mineral. Numerical simulations have been performed to define the relaxation spectrum of a reservoir rock bearing both oil and water (Talabi and Blunt, 2010). The authors described the wettability of saturated and waterflooded sandstones and sand grain packs from the mechanism that governs the surface relaxation. If one fluid relaxes similarly to its bulk relaxation, then the rock shows preference to the other fluid that relaxes faster because it interacts with the surface.

3.2.2.3 Limitations of 1D NMR: T_1 and T_2.

When comparing different rocks with similar fluids, the observed relaxation rates are proportional to *S/V*; therefore, T_1 and T_2 measurements cannot be readily used to

compare interactions between materials with differing pore geometry and pore size. When comparing the same rock with different fluids, *S/V* is affected by changes in degree of adsorption (Schoenfelder et al., 2008; D'Agostino et al., 2014). Therefore, absolute T_1 and T_2 measurements cannot be used to compare the solid-fluid interactions when more than one fluid interacts with the solid. On the other hand, the ratio of relaxation times T_1/T_2 is independent of these characteristics and is only affected by changes in the surface relaxivity and has been used to indicate the adsorption and desorption phenomena that may occur at solid fluid interfaces of porous media (Weber et al., 2009).

Another limitation of absolute T_1 and T_2 measurements in complex pore systems; such as reservoir rocks, is that different fluids cannot be separated from the T_2 alone since the water signal may overlap with the oil signal when confined in small pore spaces. In this case, the difference in the self-diffusion coefficient of each fluid, *D*, might separate the signal of water and oil. However, for T_2 less than 10 ms, it is not measurable because of hardware limitations (Jiang et al., 2013).

3.2.2.4 T_1 / T_2 ratio.

Kleinberg et al., (1993), used the T_1/T_2 ratio (determined from 1D NMR T_1 and T_2 measurements) to illustrate the changes of the transverse relaxation due to internal field gradients which are difficult to characterize. Many rock samples were investigated in order to observe the difference of T_2 from T_1. Part of the concluding remarks in their study was that when sufficiently small echo spacing is used, the shortening of T_2 at 1 to 2 MHz Larmor frequency can be minimized, and that the T_2 distribution has a similar appearance to T_1 with a slight shift of the scale, which due to microscopic field gradients cannot be eliminated. Similarly to the present study, the T_1/T_2 ratio can be determined from 2D NMR measurements; T_1-T_2 maps. In a study on dolomites and limestones from a Permian aquifer in Central Germany, the different content of iron and manganese minerals and the differences in pore classes resulted in different values of T_1/T_2 ratio (Schoenfelder et al., 2008). In other materials, McDonald et al., (2005), used the T_1/T_2 ratio as a tool to describe the chemical exchange between water and cement paste and both D'Agostino et al., (2014), and Mitchell et al., (2013), studied the T_1/T_2

ratio in order to define the adsorption strength of water on different catalysts. The strength of the interaction of the fluid with the solid is reflected in the T_1/T_2 ratio, and a high ratio is the result of the fluid adsorbing on the surface (D'Agostino et al., 2012; McDonald et al., 2005). Ozen and Sigal, 2013, observed that oil saturated organic shale cuttings had higher T_1/T_2 ratios than the water saturated. In this study the authors used the ratio T_1/T_2 to distinguish oil from water wetting the organic shale. Thus, T_1/T_2 ratios can potentially be used to define the pore fluid distribution and wettability of reservoir rocks.

3.2.2.5 *D*-T_2 maps.

Hurlimann et al., (2004), investigated the *D*-T_2 maps of chlorite bearing sandstones. This study underlined the difficulty to separate the water from the oil signal based solely on the T_1 or T_2 distributions of the rock, since the complexity of the pore size distribution of the rock prevented the identification of the pore fluid distribution. The *D*-T_2 maps proved a reliable tool to illustrate the presence of water if it is in great amount within the pore space.

Microscopic field gradients can be defined with the correlation of transverse relaxation and self-diffusion coefficient of the pore fluid in *D*-T_2 maps (Dunn et al., 2002; Flaun et al., 2005). T_2 of different fluids may overlap in the relaxation data, but the difference in their self-diffusion coefficient can separate them in such maps. *D*-T_2 maps have been used to describe the wetting phase in Bentheim and Berea sandstone and dolomites from Yates formation (Hurlimann et al., 2003). All rocks were apparently water wet, since the oil within the pores relaxed similarly to the free bulk oil, while the water was restricted on the surface. Overall, *D*-T_2 maps are a good indicator of the fluid bound on the surface of a mineral (Zielinski et al., 2010).

3.2.3 The use of NMR to determine small amounts of oil in water

Related to the fourth research objective of the present study, low field NMR spectrometry can directly measure the presence and quantities of the different fluids (water, oil, and gas) (Coates, 1999). Low field NMR spectrometry has successfully been

applied for the determination of a mixture of heavy oil and bitumen with water in emulsions in situ conditions (Allshop et al., 2001). NMR experiments conducted at the same parameters and magnetic field strength provide similar results independent of the user, equipment and software used and the results should be reproducible with high accuracy in a fluid-fluid system as illustrated in Allshop et al., (2001). NMR technique has been used for the determination of the water droplet size in water-in-oil emulsions, as they form in oil and gas pipelines (Majid et al., 2015).

4 Rock material and brines

4.1 Reservoir and quarry chalk

Chalk is a sedimentary rock of high homogeneity on the scale where physical properties are measured, and its properties fall in wide ranges. Porosity is a main determining factor for other properties. Chalk has been studied widely (e.g. Fabricius et al., 2003) and the relation between porosity, permeability, capillary entry pressure, and elastic moduli has been investigated.

The selected reservoir chalks of Tor Formation are from the Gorm field in the North Sea (Katika et al., III). Three horizontal plugs, 30 mm length and 37 mm diameter, were drilled and side and end trims were selected to investigate the solid- fluid affinity of reservoir chalk.

Two blocks of quarry chalk are studied; chalk mudstones and wackestones of Tor formation (Katika et al., I and II). Both chalks were from Stevns Klint near Copenhagen, Denmark; two different blocks (mudstone and wackestone block) from the same area but different beds. Fifteen core plugs, 50 mm length and 37 mm diameter, were drilled from the mudstone chalk and twelve core plugs, 50 mm length and 37 mm diameter, from the wackestone. Additional rock material from each block was kept for mineralogical investigation to study the effect of divalent ions on the specific surface of the grains, elasticity and pore collapse of chalk.

4.2 Berea sandstone

Berea sandstone is often used as a reference sandstone for reservoir rocks because it is relatively homogeneous and readily available (Churcher, 1991). Kaolinite is the dominant clay mineral in the Berea sandstone used in the present study. Three core plugs, 30 mm length and 37 mm diameter, and their side and end trims were selected to study the solid- fluid affinity of argillaceous sandstones (Katika et al., III).

4.3 Reservoir greensand

The studied greensand is a mixture of quartz grains and chlorite grains from the Solsort field in the North Sea (Katika et al., III). The mineral responsible for the microporosity of greensand is chlorite which is known for a high paramagnetic index (Hurlimann et al., 2004) and high stiffness (K_0 = 164.3 GPa) (Wang et al., 2001). Three horizontal core plugs, 30 mm length and 37 mm diameter, were drilled and side and end trims were selected in order to study the solid- fluid affinity of argillaceous sandstones (Katika et al., III).

4.4 Brines and oil

For the preparation of the high salinity brines related to studies on chalk from Stevns Klint (Katika et al., I and II), all salts used were dissolved in $CaCO_3$ equilibrated water (24 ppm) (Table 4.1). The density of the brines and oil was measured using a digital density meter of high accuracy (±0.001 g/cm^3).

Table 4.1. Brines used for the saturation of quarry chalk (Katika et al., I & II).

Brine used for saturation	Conc. (ppm)	Fluid density (g/cm^3)
Deionized water	-	0.997
$CaCO_3$ water	24	0.997
NaCl solution	100000	1.069
$MgCl_2$ solution	58000	1.044
$CaCl_2$ solution	68000	1.049
Na_2SO_4 solution	87000	1.071

Table 4.2. South Arne dead oil properties (Katika et al., III & IV).

Property	South Arne oil
Density (g/cm^3)	0.845
Viscosity (cP)	4.96
Total Acid Number (mg/g)	0.372
Total Base Number (mg/g)	2.03

For the study of the solid-fluid affinity of quarry and reservoir rocks, the cores were saturated with NaCl brine (30000 ppm, 1.019 g/cm^3) and dead oil from the South Arne field in North Sea (Katika et al., III). The dead oil properties are given in Table 4.2.

For the oil detection experiments series of pre-determined South Arne dead oil (Table 4.2) and synthetic seawater (1.019 g/cm^3) mixtures were used (Katika et al., IV). The composition of the seawater is shown in Table 4.3. The accuracy of four methods to quantify a known amount of oil and water was studied on the samples shown in Table 4.4. For the quantification of oil volumes using the Liquid Scintillation Analysis, oil from South Arne was doped with radiolabelled stearic acid (Table 4.5).

Table 4.3. Seawater composition used in oil detection experiments (Katika et al., IV).

Components	g/l
NaCl	18.01
$NaHCO_3$	0.17
KCl	0.75
$MgCl_2 \cdot 6H_2O$	9.15
$CaCl_2 \cdot 2H_2O$	1.91
Na_2SO_4	3.41
TDS	33.39

Table 4.4. Dead oil samples (NO) to define the accuracy of four techniques to quantify the oil volume in predetermined oil and water samples (Katika et al., IV).

Sample ID	Oil mass (g)	Oil vol. (μL)
NO-1	0.853	1007.4
NO-2	0.635	750.2
NO-3	0.422	498.2
NO-4	0.254	300.1
NO-5	0.086	102.1
NO-6	0.045	53.3
NO-7	0.021	24.6
NO-8	0.010	11.2
NO-9	0.005	5.6
NO-10	0.000	0.0

Table 4.5. Physical properties of radiolabelled stearic acid (Lide and Milne, 19)

Name: Stearic acid [1-^{14}C]	Formula: $CH_3(CH_2)_{16}{}^{14}COOH$
Physical properties	
MP (^{0}C)	68.8
BP (^{0}C)	350
Density (g/ml)	0.9408
H_2O: insoluble, EtOH, Benzene: slightly soluble, Acetone, Chloroform, CS_2 : very soluble	

5 Methods

5.1 Mineralogical composition

5.1.1 Carbonate content of chalk samples

The carbonate content of chalk was quantified by dissolving approximately 100 mg of crushed rock in hydrochloric acid (HCl) and subsequent titration with NaOH. The above-mentioned procedure was performed on the side trims of each chalk plug.

5.1.2 Insoluble residue of chalk samples

The insoluble residue (IR) in chalk, representing all the non-carbonate minerals, was determined from the selected side trims of each plug after the removal of the carbonate content by gradual dissolution in acetic acid.

5.1.3 BSEM images

Backscatter electron micrographs (BSEM) of all lithologies were recorded with a Quanta 200 (FEI) scanning electron microscope on polished thin sections of the end trims of selected core plugs.

5.1.4 X-ray diffraction

Both powdered original side trims and IR samples were analyzed by X-ray diffraction (XRD) by using Cu K-α radiation with a Philips PW 1830 diffractometer.

5.2 Soxhlet extraction cleaning

The plugs were cleaned for salt and hydrocarbons by Soxhlet extraction. The samples were refluxed by methanol to remove salts and toluene to remove the hydrocarbons. Clean plug were dried in an oven at 55°C for two days.

5.3 Porosity-Permeability

Helium porosity and Klinkenberg corrected permeability were measured on cleaned and dried plugs. Both measurements were conducted on a PoroPerm Production 2 gas porosimeter from Vinci Technologies. The bulk volume of the samples was determined utilizing mercury immersion and Archimedes' principle.

5.4 Specific surface area

The specific surface area (S_{BET}) of the side trims of all plugs with respect to weight (m^2/g) was obtained with the nitrogen adsorption method. Brunauer, Emmet and Teller (BET) inversion (Brunauer et al., 1938) was used to calculate the S_{BET} (multi-point).

The specific surface area with respect to bulk volume, S_b (1/μm) and porosity, S_ϕ (1/μm) was calculated using Equations 5.1 and 5.2, respectively. ,

$$S_b = S_{BET}\rho_g(1-\phi), \tag{5.1}$$

$$S_\phi = S_b / \phi. \tag{5.2}$$

where ϕ is the porosity and ρ_g (g/cm^3) the grain density.

The BET measurements were performed, using the Autosorb iQ gas sorption system from Quantachrome Instruments.

By using Kozeny's theory (Mortensen et al., 1998), liquid permeability, *k* was calculated from the following equation, where *c* is Kozeny's constant:

$$k = c\phi^3 / S_b^{\,2}\ \text{, where, } c = \left(4\cos\left(\frac{1}{3}\arccos\left(\phi\frac{8^2}{\pi^3}-1\right)+\frac{4}{2}\pi\right)+4\right)^{-1}. \tag{5.3}$$

5.5 Capillary pressure curves

The mercury capillary pressure test provided information concerning the throat size distribution of the dry rocks. The experiments were performed on side trims from the selected material utilizing a Poremaster® PM 33-GT-12, mercury porosimetry analyzer. Conversion of pressure data to throat size distribution was performed with the

Poremaster software from Quantachrome™ Instruments. Mercury was injected with pressure up to 60000 psi in small chips of the rock (10 g).

5.6 Ultrasonic data

Elastic wave velocities were measured at ambient temperature by placing the dry plugs between two pistons of a loading frame under uniaxial unconfined compressive conditions at 2 MPa. After fluid saturation the velocities were measured under the same conditions. The compressional and shear wave velocity were measured by recording the travel time of a transmitted ultrasonic wave at 200 kHz through the sample. The experimental setup applied in Katika et al., II is shown in Figure 5.1.

5.7 Electrical resistivity

The electrical resistance of the saturated cores was measured at ambient temperature simultaneously with velocity, from a variable resistor connected in series with the sample in a 1 kHz AC circuit of 1 volt power supply (Figure 5.1).

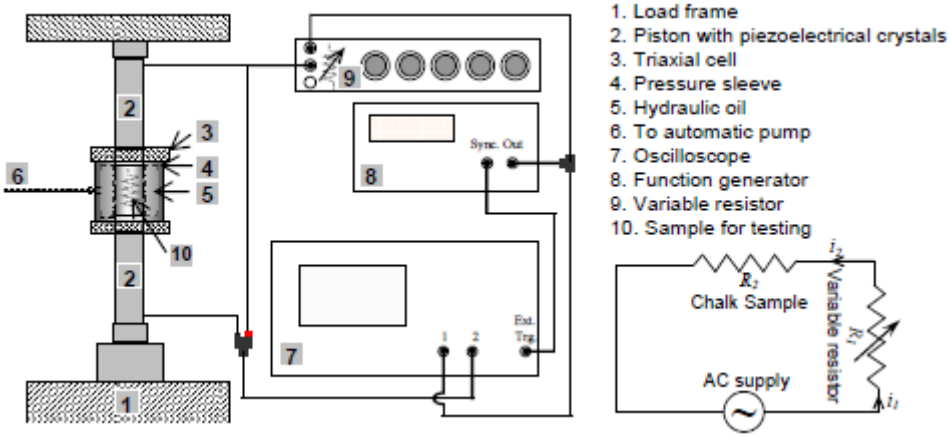

Figure 5.1 Experimental setup for sonic velocity and resistivity measurements (Alam, 2011)

5.8 Low-field NMR measurements

5.8.1 T_1 distribution

The T_1 distribution of the saturated cores was acquired at a 2 MHz Magritek Rock Core Analyzer™. The longitudinal relaxation was acquired using Inversion Recovery Free

Induction Decay (IRFID) (Dunn et al., 2002) using 30 logarithmically spaced wait times ranging from 0.1 to 10000 ms. All measurements were converted to porosity and the signal amplitude was calibrated according to the signal amplitude of the saturating fluid.

5.8.2 T_2 distribution

The T_2 distribution of the saturated cores was acquired utilizing two different instruments; 2 MHz MagriteK Rock Core Analyzer^{TM} at Colorado School of Mines (Katika et al., III) and GeoSpec NMR core analyser at 2.25 MHz at DTU (Katika et al., I, II and IV). The transverse relaxation was acquired using the Carr-Purcell, Meiboom and Gill (CPMG) pulse sequence (Dunn et al., 2002). Measurements were performed at Signal to Noise Ratio (SNR) equal to 250. The polarization time was selected at 5 s, number of echoes at 16000, and the echo spacing (TE) at 100 μs. All measurements were converted to porosity and the signal amplitudes were calibrated according to the signal amplitude of the saturating fluid.

5.8.3 T_1-T_2 and D-T_2 measurements

T_1-T_2 and D-T_2 NMR mapping of the saturated cores was conducted using similar acquisition parameters as in 1D T_1 and T_2 measurements for the transverse relaxation (Sun and Dunn, 2002). A combination of CPMG and Pulsed Gradient Spin Echo (PGSE) experiments were conducted for D-T_2 measurements (Latour et al., 1993). A pair of gradient pulses of duration, δ, 1.5 ms and separation, Δ, 10 ms, was applied on both sides of the 180 degree pulse. The strength, g, of the gradient pulses was incremented between experiments. The raw 2D data were analyzed using a two dimensional distribution function and an inverse Laplace transform to generate the 2D maps (Hürlimann et al., 2003; Venkataramanan et al., 2002, and Song, 2010).

5.9 Oil detection in effluents

5.9.1 The Image analysis method

High resolution images were taken and analyzed with the help of the digital analysis software ImageJ in order to detect the oil volume in pre-determined oil and water samples (Katika et al., IV).

5.9.2 The UV/Visible spectroscopy analysis method

The NO samples and samples for the standard curve were treated using the UV/visible spectroscopy as described by Evdokimov et al., (2003a, b), in order to detect the oil volume in pre-determined oil and water samples (Katika et al., IV).

5.9.3 The Liquid Scintillation Counting method

For the LSC method, the oil in samples with pre-determined amount of oil and water was doped with low-concentration, radiolabeled stearic acid [$^{-14}$C], which is fully dissolvable in the oil and insoluble in water. All the samples were analyzed using the scintillation counter (Hidex 300 SL, 1414 LS Counter) (Katika et al., IV).

5.10 Saturation

For the case of full water and oil saturation, batches one and two, the samples were placed in a desiccator and vacuum was created by an air pump while fluid was poured into the bottom of the vessel gradually until the samples were covered with fluid. For the case of irreducible water saturation, batch three was firstly fully saturated with salt water. The water of chalk was removed while oil was flushed into the pore space till no more water is expelled from the rock. In order to achieve irreducible water saturation for Berea sandstone and greensand, the method of porous plate desaturation was used (Gray et al., 1993). All samples spent 12 hours in a pressure vessel at 1600 psi fully covered with oil in order to ensure full saturation. Complete saturation was verified by using the dry and saturated weight, grain volume by helium expansion, water and oil density.

6 Rock properties

6.1 Chalk from the Gorm Field properties

Chalk from the Gorm Field has a bimodal grain size distribution, but the pore space is homogeneous, as illustrated in the pore throat distributions from MICP and BSEM images (Figure 6.1). The mineral composition is shown in Table 6.1. The petrophysical properties of the core plugs are shown in Table 6.2. Chalk from the Gorm Field was saturated with oil, water and oil and water at irreducible water saturation state (Table 6.3) in order to investigate the solid-fluid affinity of the rock (Katika et al., III).

Table 6.1. Mineral composition of the studied material (-M- representing the major components and –m- the minor components from the XRD analysis)

Mineral	Gorm Field Chalk	Stevns Klint Chalk	Berea Sandstone	Solsort field Greensand
Quartz	m	m	M	M
K-Feldspar	m	m	m	traces
Calcite	M	M	-	traces
Kaolinite	m	m	M	m
Chlorite	m	-	-	M
Illite	-	-	-	m
Smectite	-	m	-	-

Table 6.2. Petrophysical properties of chalk from the Gorm field, Berea sandstone and greensand from the Solsort field (Katika et al., III).

Sample ID	Depth (ft-md)	Lithology	Grain Density (g/cm^3)	Helium Porosity (fraction)	Klink. permeability (mD)	S_{BET} (m^2/g)	NMR-T_2 Porosity (fraction)
N-3X-T1	6901	Chalk	2.70	0.35	4.16	1.4	0.36
N-3X-T2	6901	Gorm	2.70	0.35	4.16	1.4	0.36
N-3X-T3	6995	field	2.70	0.34	6.07	1.2	0.35
BS-T1	-	Berea sandstone	2.67	0.20	99.7	1.3	0.20
BS-T2	-		2.66	0.20	85.4	1.3	0.20
BS-T3	-		2.66	0.22	196.5	1.2	0.22
GSD-T1	3014	Greensand	2.73	0.32	117.6	8.7	0.32
GSD-T2	3708	Solsort	2.72	0.32	116.1	8.7	0.32
GSD-T3	3710	field	2.73	0.32	111.4	8.7	0.33

Table 6.3. Saturation of chalk from the Gorm field, Berea sandstone and greensand from the Solsort field (Katika et al., III).

Sample ID	Water saturation, %	Oil saturation, %	Total saturation, %
N-3X-T1	100	0	100
N-3X-T2	0	98	98
N-3X-T3	40	60	100
BS-T1	96	0	96
BS-T2	0	97	97
BS-T3	17	83	100
GSD-T1	100	0	100
GSD-T2	0	100	100
GSD-T3	46	54	100

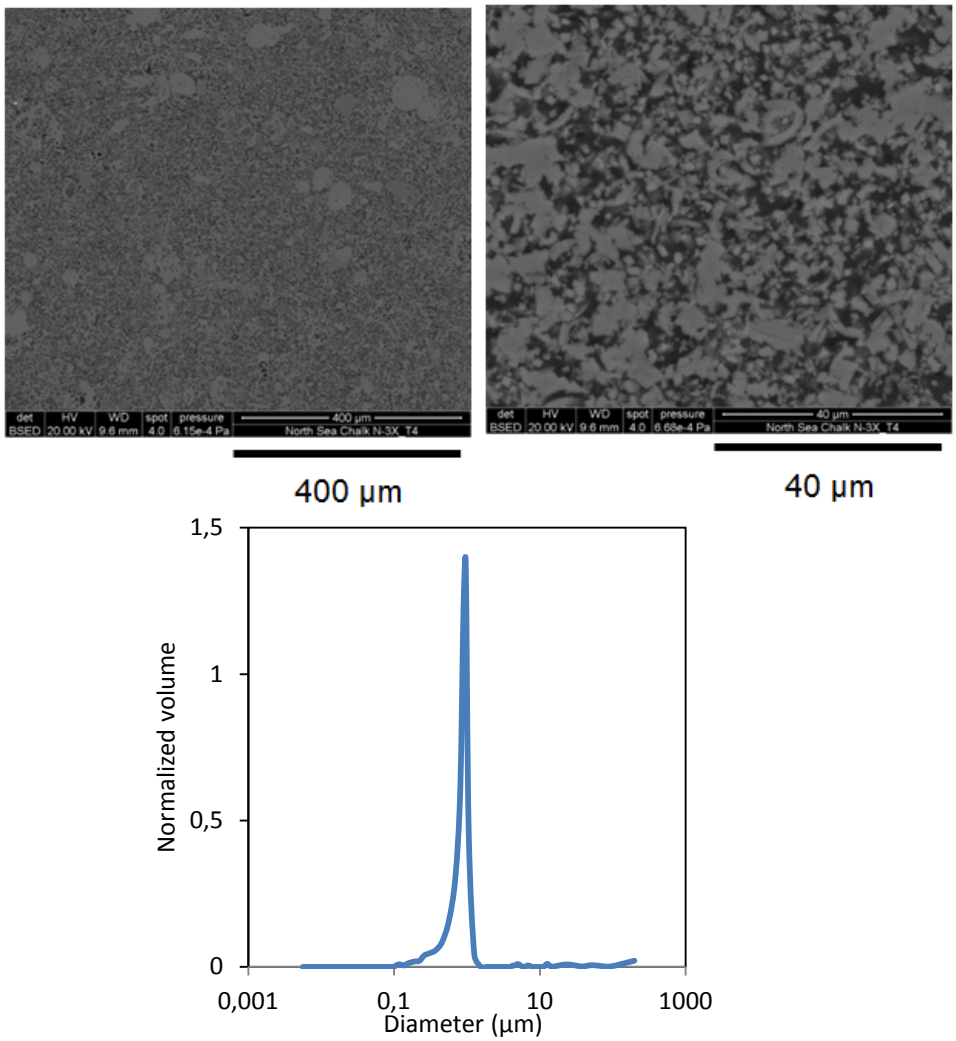

Figure 6.1. Top: BSEM image in low and high resolution, and bottom: throat size distribution from MICP for the chalk from the Gorm field well, 6995 ft., md.

6.2 Chalk from Stevns Klint properties

Chalks from Stevns Klint have a bimodal grain size distribution, but the pore space is more homogeneous, as illustrated in the pore throat distributions from MICP and BSEM images (Figures 6.2 and 6.3). The carbonate content and the clay content has been determined and shown in Table 6.1. Mudstone and wackestone chalk are both rather homogeneous with similar pore sizes. The difference in texture can be attributed to the presence of intrafossil porosity in the wackestone samples observed both in the BSEM image and throat size distribution from MICP (Figure 6.3).

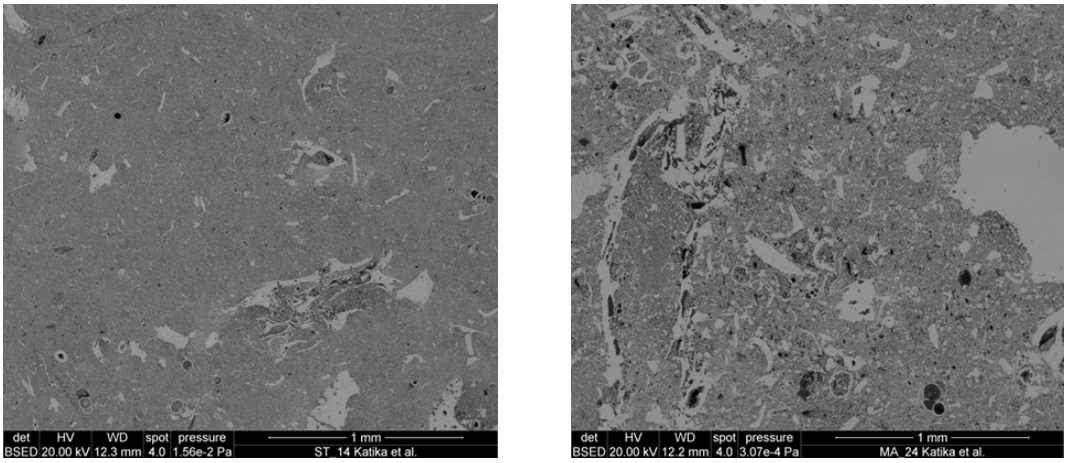

Figure 6.2. Backscatter electron micrographs of chalk sample with mudstone texture (left), and chalk sample with wackestone texture (right) (Katika et al., I).

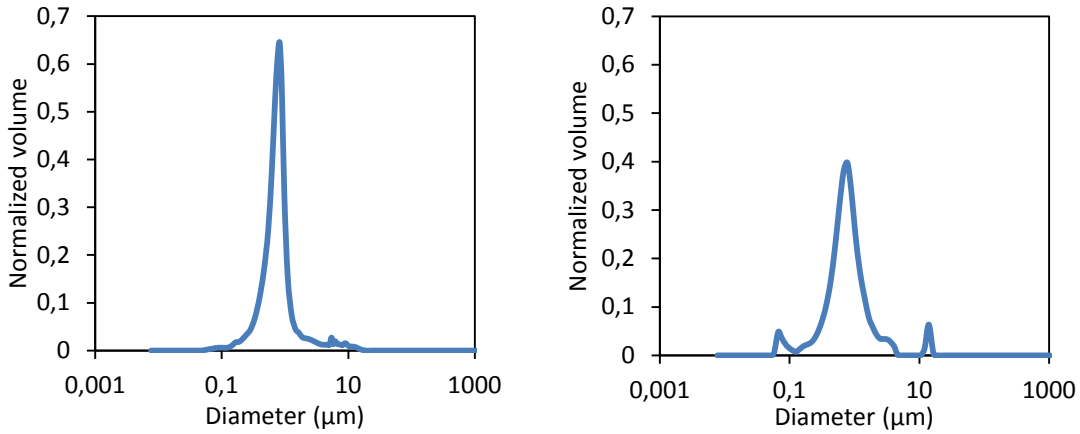

Figure 6.3. The throat size distribution of chalk from Stevns Klint with mudstone texture (left) and wackestone texture (right).

The petrophysical properties of the plugs drilled from the mudstone and wackestone block are shown in Table 6.4 and Table 6.5 respectively. Chalk from Stevns Klint was

saturated with high salinity brines with specific ion content (Table 6.6) in order to investigate the effect of potential determining ions and high salinity brines on the specific surface, elasticity and pore collapse of the rock (Katika et al., I and II).

Table 6.4. Core plug properties from the mudstone chalk from Stevns Klint (Katika et al., I).

Core ID	Bulk volume (cm^3)	Grain density (g/cm^3)	Helium porosity (%)	S_ϕ ($1/\mu m$)
ST-02	54.67	2.71	42	6.4
ST-03	55.03	2.71	42	6.4
ST-06	55.54	2.71	41	6.6
ST-11	53.34	2.71	42	6.4
ST-12	53.68	2.70	42	6.3
ST-13	56.26	2.71	41	6.6
ST-15	54.81	2.71	42	6.4
ST-16	53.81	2.71	43	6.1
ST-17	54.96	2.70	43	6.1
ST-19	55.53	2.71	43	6.1
ST-20	55.29	2.71	42	6.4
ST-21	54.26	2.71	41	6.6
ST-22	52.68	2.70	41	6.6
ST-23	55.55	2.71	43	6.1
ST-24	55.07	2.71	43	6.1

Table 6.5. Core plug properties from the wackestone chalk from Stevns Klint (Katika et al., I).

Core ID	Bulk volume (cm^3)	Grain density (g/cm^3)	Helium porosity (%)	S_ϕ ($1/\mu m$)
MA-01	52.54	2.71	38	7.1
MA-02	50.81	2.71	38	7.1
MA-03	53.18	2.70	38	7.0
MA-04	51.75	2.70	38	7.0
MA-05	50.93	2.70	38	7.0
MA-06	51.36	2.70	36	7.7
MA-07	50.69	2.70	39	6.8
MA-09	50.37	2.70	38	7.0
MA-10	50.04	2.70	37	7.4
MA-14	51.98	2.70	37	7.4
MA-15	49.66	2.70	38	7.0
MA-16	50.22	2.70	38	7.0
MA-17	51.16	2.70	37	7.4
MA-18	50.35	2.70	38	7.0
MA-19	51.14	2.70	38	7.0

Table 6.6. Saturation of chalk from Stevns Klint with mudstone (ST-samples) and wackestone texture (MA-samples) (Katika et al., I).

Core ID	Brine used for saturation	Conc. (g/L)	Fluid density (g/cm^3)	Sw (%)	Core ID	Brine used for saturation	Conc. (g/L)	Fluid density (g/cm^3)	Sw (%)
ST-02	Deionized water	-	0.997	96	MA-01	Deionized water	-	0.997	99
ST-03				96	MA-02				100
ST-06				96	MA-03				99
ST-11	NaCl solution	100	1.069	97	MA-04	NaCl solution	100	1.069	99
ST-12				95	MA-05				97
ST-13				95	MA-09				99
ST-15	$MgCl_2$ solution	58	1.044	95	MA-06	$MgCl_2$ solution	58	1.044	97
ST-16				95	MA-09				99
ST-17				95	MA-10				98
ST-19	$CaCl_2$ solution	68	1.049	97	MA-14	$CaCl_2$ solution	68	1.049	98
ST-20				96	MA-15				97
ST-21				99	MA-16				98
ST-22	Na_2SO_4 solution	87	1.071	100	MA-17	Na_2SO_4 solution	87	1.071	96
ST-23				97	MA-18				100
ST-24				95	MA-19				99

Additional plugs from Stevns Klint were saturated to illustrate the effect of $CaCO_3$ water (24 ppm) on the specific surface of the rock. Information concerning the physical properties and the saturation of those samples is given in Table 6.7 (Katika et al., I).

Table 6.7. Physical properties and information concerning the saturation of the chalk samples from Stevns Klint saturated with $CaCO_3$ equilibrated water (Katika et al., I).

Core ID	Bulk volume (cm^3)	Grain density (g/cm^3)	Helium porosity (%)	S_ϕ ($1/\mu m$)	Fluid density (g/cm^3)	Sw (%)
ST-07	56.21	2.71	42	6.4	0.997	95
ST-08	55.02	2.71	42	6.4		95
ST-09	54.70	2.71	42	6.4		95

6.3 Berea sandstone properties

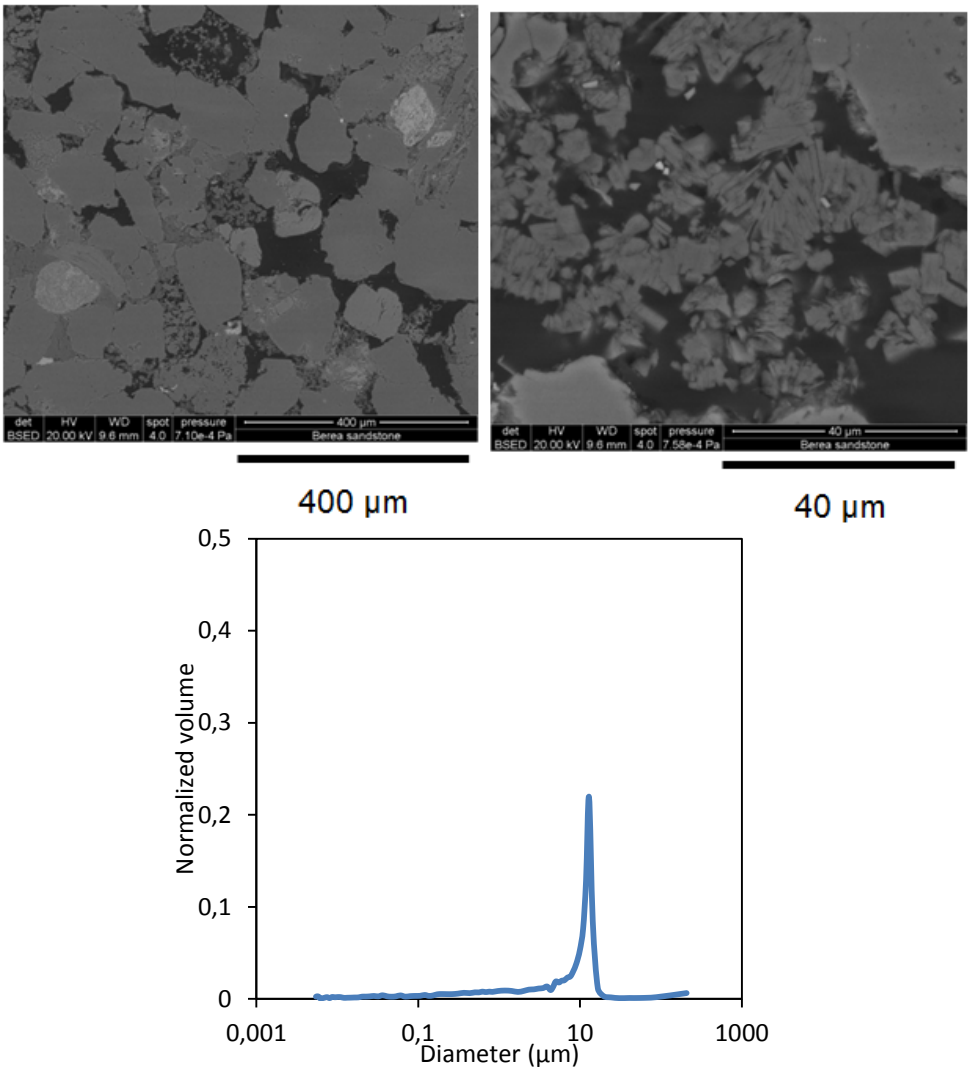

Figure 6.4. Top: BSEM image in low and high resolution, and bottom: throat size distribution from MICP for the Berea sandstone (Katika et al., III).

The BSEM image of the Berea sandstone in Figure 6.4 shows that it is rich in quartz and part of the pore space contains loose kaolinite (Table 6.1). The pore throat distribution from MICP shows the main peak reflecting large pores and a long tail in smaller throats among the clay minerals present in the core (Figure 6.4). The petrophysical properties of the selected plugs are shown in Table 6.2 and the saturation with oil, water and oil and water at irreducible water saturation state are shown in Table 6.3 (Katika et al., III).

6.4 Greensand from the Solsort field properties

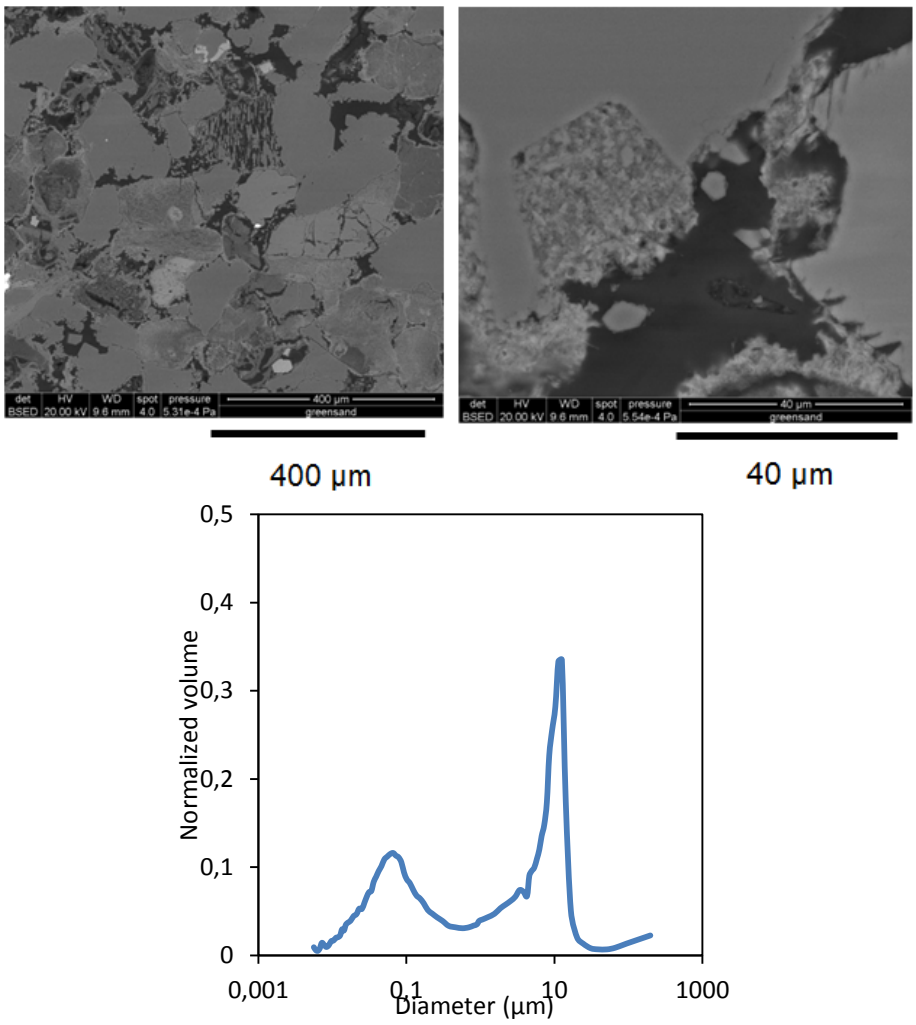

Figure 6.5. Top: BSEM image in low and high resolution, and bottom: throat size distribution from MICP for the chloritic greensand, Solsort field, 3710.13 ft. depth-md (Katika et al., III).

The greensand is rich in quartz and chlorite grains as well as pore filling chlorite (Table 6.1). Porosity occurs at two scales: large pores between grains and small pores within the chlorite grains as observed in Figure 6.5. The petrophysical properties of the selected plugs are shown in Table 6.2 and the saturation with oil, water and oil and water at irreducible water saturation state (Table 6.3) (Katika et al., III).

7 First research objective - Katika et al., I
Changes in specific surface of chalk, caused by saturation with porewater bearing divalent ions

In this chapter we present data from petrophysical investigations of chalk from Stevns Klint to illustrate the interaction of divalent ions with the surface of this porous medium with the use of low field NMR spectrometry. Laboratory experiments were conducted on core plugs saturated with different fluids to evaluate the effect of salinity and specific ions (Na^{1+}, Mg^{2+}, Ca^{2+} and SO_4^{2-}) on the surface-to-volume ratio of quarry chalk samples with two different textures. The T_2 distributions of the fully saturated chalk samples were studied in order to define how they are affected by the presence of individual ions. Three different mechanisms were investigated; changes in the properties of brines before and after contact with chalk, changes in the specific surface of mudstone chalk saturated with divalent ions and changes in the specific surface of wackestone chalk saturated with the same brines as the mudstone chalk.

7.1 Brines before and after contact with chalk

$MgCl_2$ and $CaCl_2$ salts were mixed with $CaCO_3$ equilibrated water, and their reaction was observed with the use of low field NMR spectrometry. Two samples were prepared and their T_2 was measured every few hours, till a shift to lower relaxation times occurred due to a precipitation reaction that took place within the solution. In the case of the Ca-rich brine a few crystals were visible in the bottom of the beaker where the salt was mixed with the $CaCO_3$ equilibrated water a few minutes after the dissolution of the salt. The results of those measurements are shown in Figure 7.1. In both samples the T_2 distribution stopped shifting to lower times after 100 hours. The shift of the T_2 curve happened faster for the case of the Ca-rich brine. Since these brines were later used for the saturation of our samples they were filtered in order to remove as many precipitants as possible. Further precipitation took place in the solutions during the saturation.

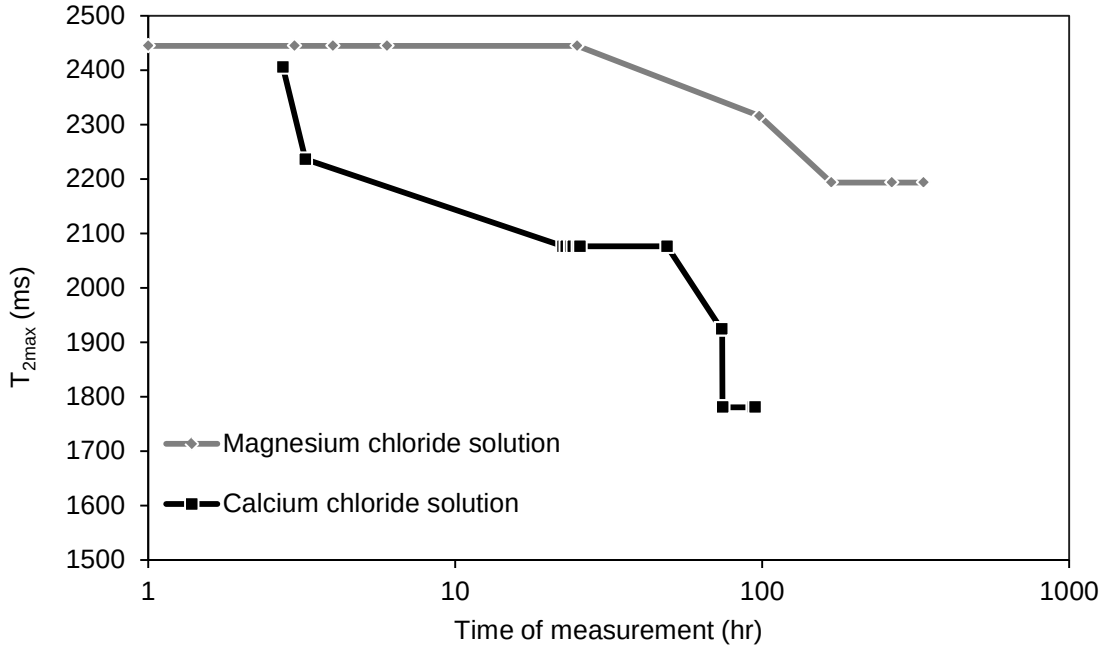

Figure 7.1. Observed precipitation reaction for the cases of $MgCl_2$ and $CaCl_2$ dissolved in $CaCO_3$ water. On the y-axis is shown the maximum value of the T_2 distrbution for every measurement. On the x-axis it is the time of each measurement; the solution was prepared at time zero, while it required approximately 15 minutes to finish the first NMR measurement (Katika et al., I).

Low field NMR spectrometry measurements were performed on the brines used for the saturation, after they spend seven days in vacuum conditions along with the chalk samples. In addition to those brines we prepared the same brines (sodium chloride solution, magnesium chloride solution, calcium chloride solution and sodium sulphate solution) with the same ionic strength (1.83 mol/L) but this time the salts were dissolved in deionized water. Figure 7.2a presents the T_2 distribution of the brines prepared with deionized water. Figure 7.2a illustrates that when no precipitation takes place the T_2 curve of the brine is always similar to the T_2 curve of the deionized water. In the cases of all sodium chloride solutions and when the salts of $MgCl_2$, $CaCl_2$ and Na_2SO_4 where dissolved in deionized water there is no extra surface inside the fluids to speed up the relaxation. Changes in the amplitude of those curves are due to changes in the amount of water molecules within the samples. Figure 7.2b, illustrates the T_2 of the bulk free brines used in the saturation. As previously observed in Figure 7.1, precipitation takes place when ions like Ca^{+2} and Mg^{+2} come in contact with carbonate ions. The T_2 of the

brines with precipitants ($MgCl_2$, $CaCl_2$ and Na_2SO_4 brines), separate from the T_2 of deionized water and NaCl solution.

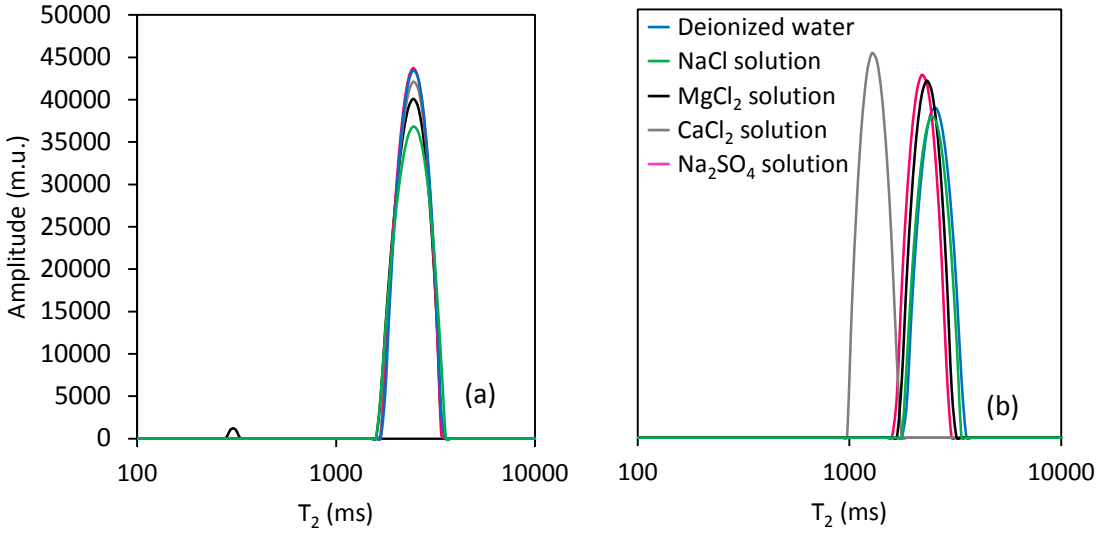

Figure 7.2. The T_2 relaxation of (a) 20 ml fluid samples of the solutions based in deionized water and (b) 20 ml fluid samples of the solutions used for the saturation. In case (a) no carbonates are present inside the fluid. In case (b) the salts where dissolved in water that contained calcium and carbonate ions and they spend seven days under vacuum conditions with the chalk for the saturation. The T_2 relaxation time is given in milliseconds on the x-axis while the amplitude is normalized in machine units on the y-axis (Katika et al., I).

The T_2 distributions of the brines used for the saturation show that excess surface is generated in the fluid when magnesium, calcium and sulphate ions are in contact with the free carbonates that exist in the $CaCO_3$ equilibrated water. This excess surface resulted in faster relaxation since the surface relaxation mechanism was introduced to the rather slow bulk relaxation of the free fluid. As a result, the water bearing precipitants obtains faster relaxation than the free fluid. The T_2 distributions show that even the smallest amount of calcium and carbonate in the water can contribute to the creation of magnesium- and calcium carbonates as well as calcium sulphate that are responsible for the creation of excess specific surface within the fluid. Checking the signal of the brines in Figure 7.2b, we can observe that the precipitants within the calcium chloride solution lead to faster relaxation than the precipitants within the magnesium chloride solution. This could be an indication of their quantity and size; more and smaller precipitants create more surface within the bulk fluid causing the molecules to relax faster.

7.2 Wackestone quarry chalk saturated with divalent ions

Figure 7.3 presents the averaged T_2 distributions (average of three core plugs saturated with the same brine) obtained from the plugs from the wackestone chalk after the saturation. From these curves we can identify two connected pore spaces. The first peak of those curves represents the typical relaxation for the brine in the pore space of chalk; just a few micrometres, and the second peak represents the relaxation of the fluid that exists in intra fossil porosity. In that case the fluid is freer and requires longer time to relax. From the derived average T_2 curves we can conclude that saturation with Mg-rich brines leads to faster relaxation of the protons than Ca and SO_4-rich brines.

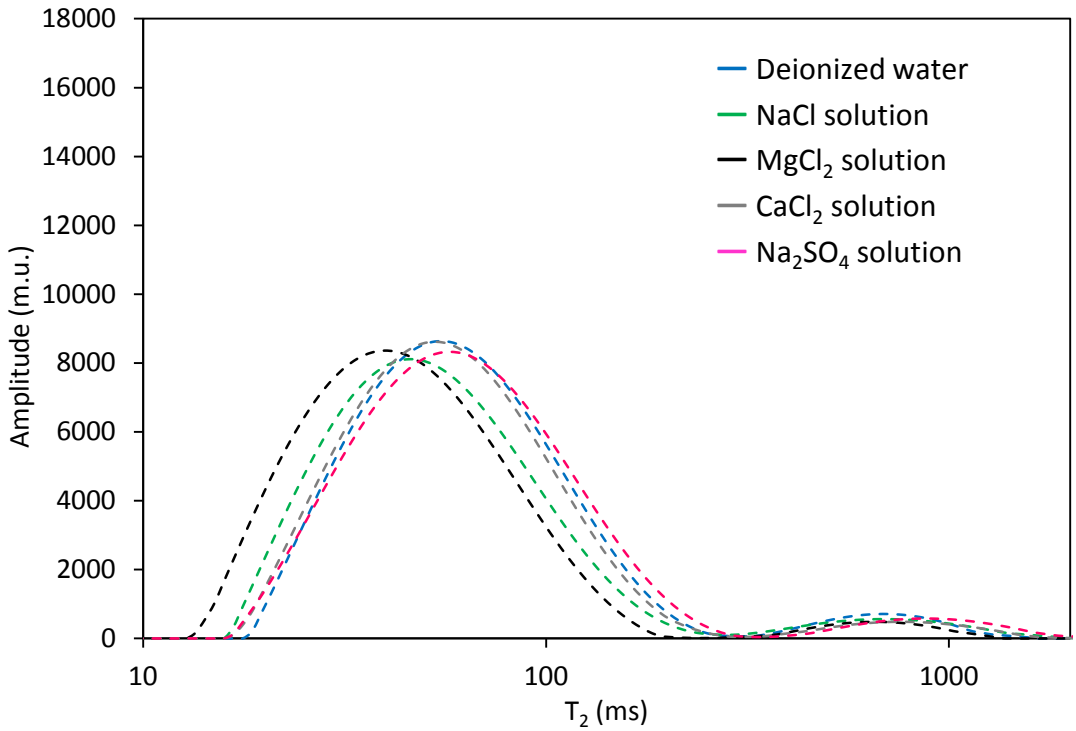

Figure 7.3. The average T_2 distribution of the saturated wackestone chalk samples. The T_2 relaxation time is given in milliseconds on the x-axis while the amplitude is normalized in machine units on the y-axis (Katika et al., I).

7.3 Mudstone quarry chalk saturated with divalent ions

Figure 7.4 presents the averaged T_2 distributions (average of three core plugs saturated with the same brine) obtained from the plugs from mudstone chalk after the saturation so as to illustrate the effect of the deionized water and each ion (Na^{1+}, Mg^{2+}, Ca^{2+} and SO_4^{2-}) on quarry chalk. From the T_2 distributions we can observe that saturation with

deionized water, $CaCO_3$ water and Na-rich water results in similar T_2-distribution. By contrast saturation with Mg-rich brines leads to faster relaxation of the protons and saturation with Ca and SO_4-rich brines leads to slower relaxation than the deionized water.

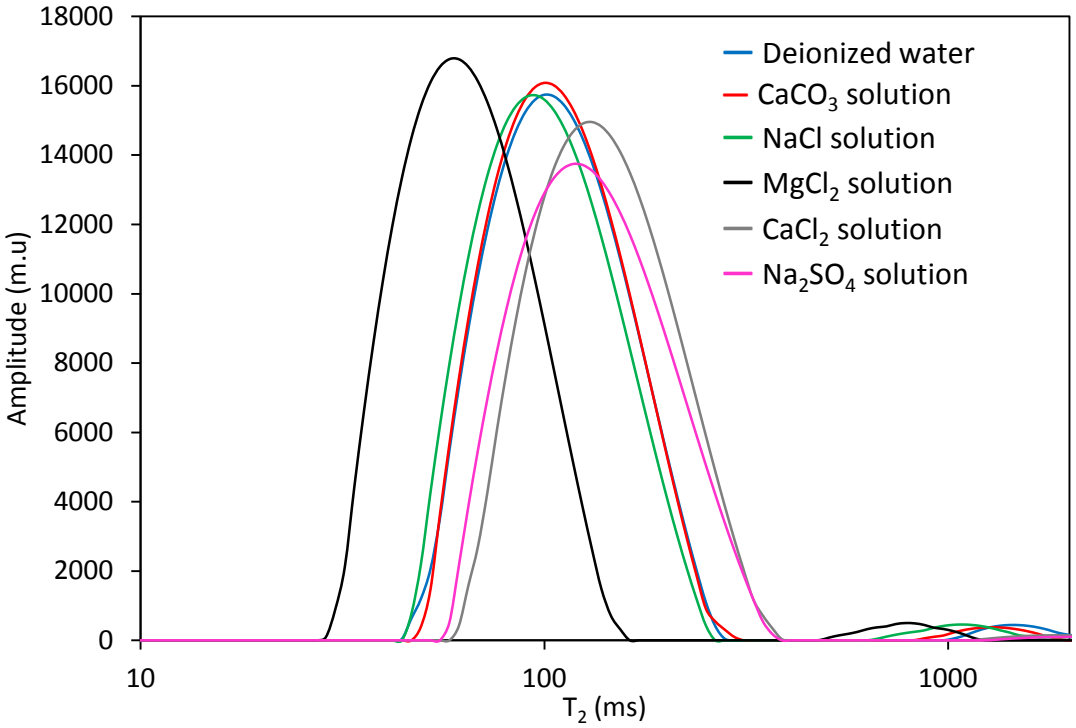

Figure 7.4. The average T_2 distribution of the saturated mudstone chalk rocks. Each of the lines represents the average line of the three cases with the same colour from Figure 4. The T_2 relaxation time is given in milliseconds on the x-axis while the amplitude is normalized in machine units on the y-axis (Katika et al., I).

As inferred in earlier studies (eg. Madland et al., 2011), saturation of carbonates with divalent ions leads to precipitation reactions that might change the surface-to-volume ratio and as a result affect the transverse relaxation time. The surface relaxivity was obtained for the deionized water saturated plugs from equation 3.4. This value is independent of any surface reactions that may have occurred after the saturation with divalent ions. If we consider that the surface relaxivity does not change after the saturation, and the shifts in the T_2 distribution are only due to changes in the surface-to-volume ratio we can calculate the specific surface of the plugs after the saturation with divalent ions. We obtained, $\rho_2 = 1.5$ μm/s for the ST-samples and $\rho_2 = 2.5$ μm/s for the MA-samples saturated with deionized water and recalculated the specific surface of the pore space for saturation with Mg^{2+}, Ca^{2+} and SO_4^{2-} ions (Table 7.1).

Table 7.1. Surface-to-volume ratio after the saturation if the surface relaxivity is not affected by the presence of divalent ions.

Core ID	Brine used for saturation	S_ϕ in dry conditions (1/μm)	S_ϕ in wet conditions (1/μm)	Core ID	Brine used for saturation	S_ϕ in dry conditions (1/μm)	S_ϕ in wet conditions (1/μm)
		ρ_2=1.5 μm/s				ρ_2=2.5 μm/s	
ST-15	$MgCl_2$ solution	6.2	11.1	MA-06	$MgCl_2$ solution	6.9	9.5
ST-16		6.1	10.7	MA-09		7.1	9.5
ST-17		6.1	10.1	MA-10		7.2	10.6
ST-19	$CaCl_2$ solution	6.1	5.0	MA-14	$CaCl_2$ solution	7.2	8.1
ST-20		6.2	4.9	MA-15		7.1	6.5
ST-21		6.4	4.9	MA-16		7.1	8.1
ST-22	Na_2SO_4 solution	6.4	5.1	MA-17	Na_2SO_4 solution	7.2	6.9
ST-23		6.1	5.2	MA-18		7.0	6.9
ST-24		6.1	5.1	MA-19		7.0	6.9

As observed the surface-to-volume ratio increases in all cases after the saturation with Mg-rich brines while reduces after the saturation with Ca and SO_4-rich brines for the case of ST-samples. Possibly the precipitants of magnesium bearing carbonates remain in the pore space of the medium increasing the specific surface, while the calcium and sulfate cover the surface of the grains and as a result reduce the specific surface. In MA-samples, Ca and SO_4-rich brines resulted in negligible differences in the surface to volume ratio after the saturation.

8 Second research objective - Katika et al., II
The effect of divalent ions on the elasticity and pore collapse of wackestone quarry chalk

This chapter discusses the elasticity and pore collapse mechanisms of chalk under the presence of potential determining ions used in waterflooding experiments and reservoir injection. The effect of pore water composition on the elasticity and strength of twelve chalk plugs was evaluated by mechanical testing. Petrophysical measurements, including low field NMR spectrometry, illustrated the interaction of individual ions with the surface of this porous medium. It is observed that divalent ions in high concentration affect the elasticity of chalk. High salinity and especially potential determining ions (Mg^{2+}, Ca^{2+} and SO_4^{2-}) weaken the rock and promote pore collapse at lower stresses as observed by rock mechanical tests. Low field NMR spectrometry data illustrated precipitation only in the pore space of chalk saturated with Mg-rich brine.

8.1 The effect of divalent ions on the elasticity of chalk

In order to compare fluid effects on samples saturated with various brines, the compressional wave moduli of the plugs in dry and saturated conditions are presented in Figure 8.1. In the same figure, the iso-frame curves are also indicated. The chalk samples in dry conditions have minor differences in their compressional wave moduli and iso-frame value. After the saturation, differences can be observed in the iso-frame value of the samples due to the effect of each ion on the elasticity of the rock. When the chalk samples are saturated with either deionized water or sodium chloride solution the iso-frame value decreases less than in the cases of chalk saturated with Mg, Ca or SO_4-rich brines. Even though the samples saturated with deionized water or NaCl solution have high compressional wave modulus in the dry state, the difference among dry and wet compressional wave moduli is relatively large when the saturating fluid contains divalent ions. So, for the cases of saturation with calcium and magnesium chloride solution there is indication of relative softening of the rock.

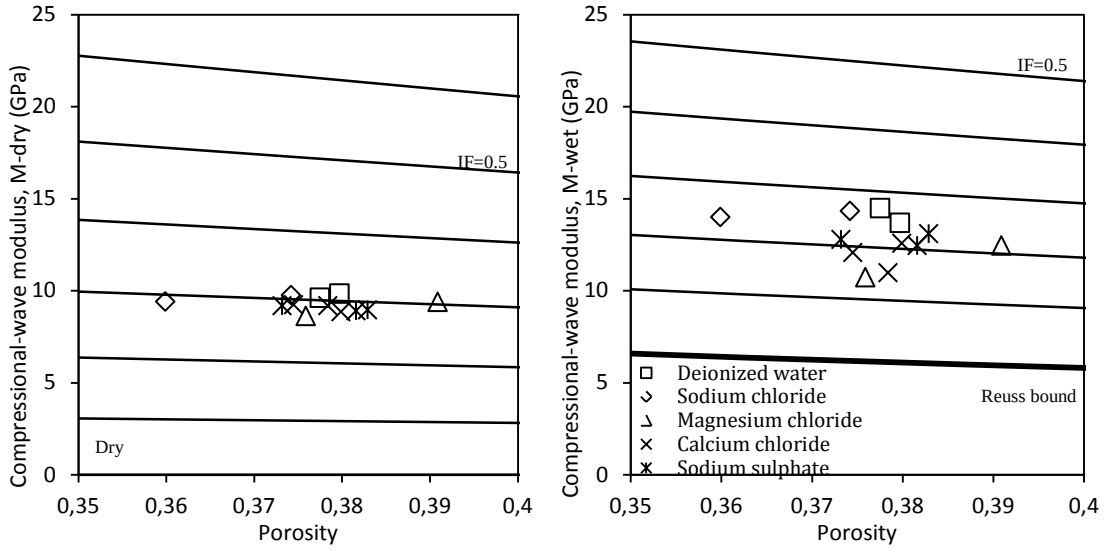

Figure 8.1. P-wave moduli as calculated from compressional wave velocity and density versus porosity for water dry and saturated chalk. Iso-frame curves are shown in intervals of 0.1 starting from 0 (Reuss bound) (Katika et al., II).

The shear modulus was derived from the P-wave modulus and iso-frame modelling as shown in Figure 8.2. Similarly to the compressional moduli, the chalk samples in dry condition have minor differences in their shear wave moduli and iso-frame value, whereas, the iso-frame values in wet conditions have higher dispersion due to the effect of each ion on the elasticity of the rock.

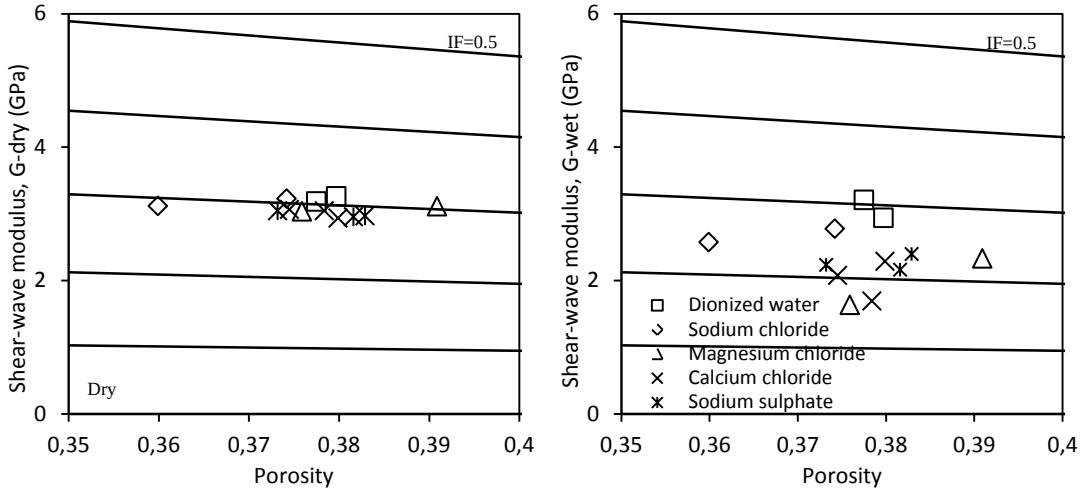

Figure 8.2. S-wave moduli as derived from P-wave moduli and iso-frame modeling versus porosity for dry and brine saturated chalk. Iso-frame curves are shown in intervals of 0.1 starting from 0 (lowest) (Katika et al., II).

8.2 The effect of divalent ions on the pore collapse of chalk

Figure 8.3 presents the stress–strain curves for the twelve uniaxial strain compression tests performed on the saturated chalk. These curves show the loading and unloading cycles the plugs were subjected to, and provide information concerning the pore collapse stress as marked on the figures. The pore collapse is determined and marked with a dot sign in Figure 8.3. Since some plugs broke during loading, in Figure 8.3 are shown two plugs saturated with deionized water (first row), two plugs saturated with sodium chloride solution (second row), two core plugs saturated with magnesium chloride solution (third row), three core plugs saturated with calcium chloride solution (fourth row), and three core plugs saturated with sodium sulfate solution (fifth row).

V_P increases when increasing stress in the beginning, then the rate of increment decays before the pore collapse (after which the V_P falls), as presented in Figure 8.4. Each graph in Figure 8.4 contains the plugs saturated with the same brine, as presented in Figure 8.3; two plugs saturated with deionized water, two plugs saturated with sodium chloride solution, two core plugs saturated with magnesium chloride solution, three core plugs saturated with calcium chloride solution and three core plugs saturated with sodium sulfate solution. The unloading cycles are disregarded and the y-axis shows the P-wave wave velocity while increasing the axial stress. After pore collapse the P-wave velocity decreases with increasing stress. The behavior of the V_P indicates that the reading of pore collapse is consistent with V_P.

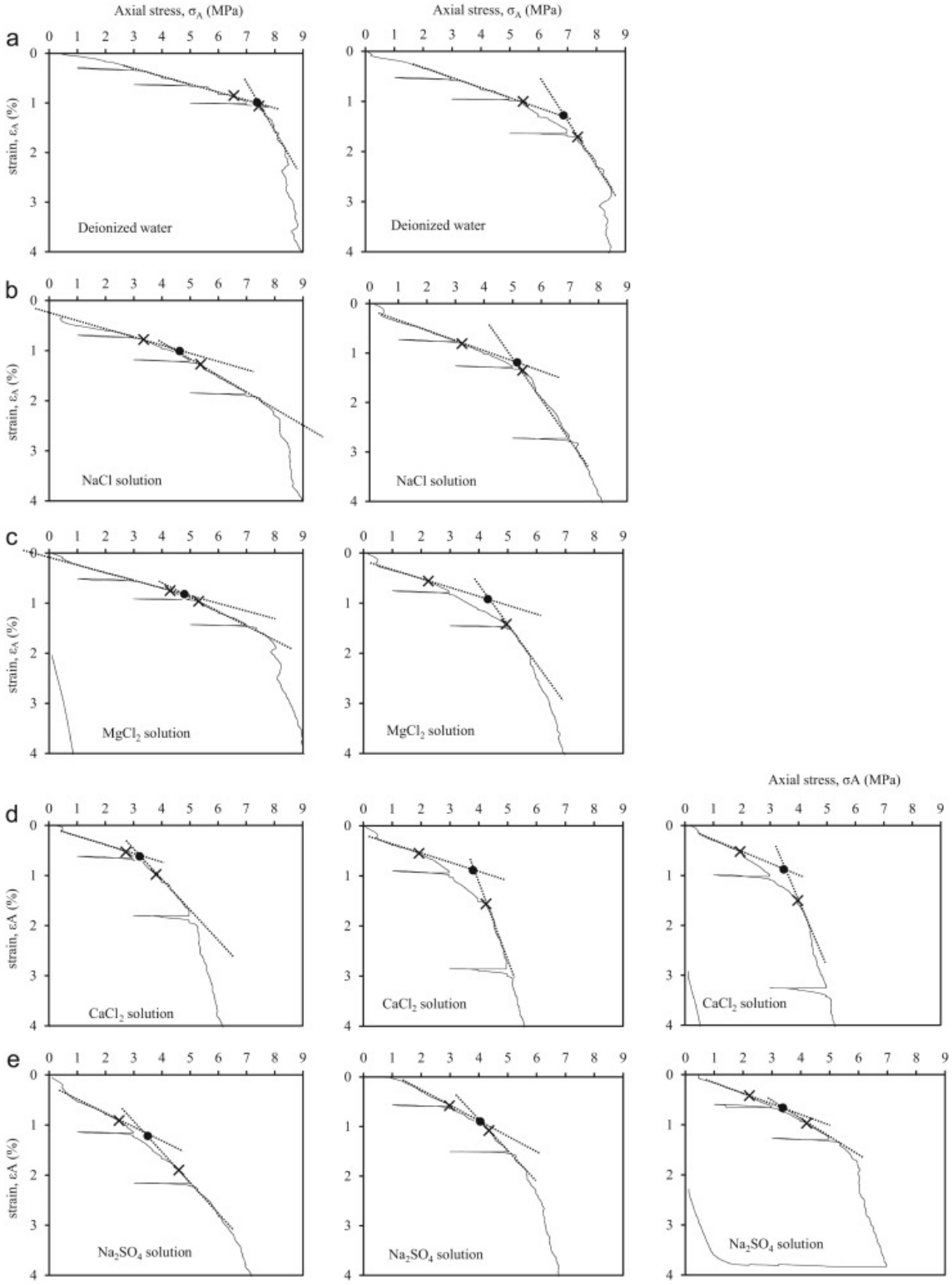

Figure 8.3. Loading curves for the chalk from Stevns Klint. All diagrams represent the stress-strain relationship with the reading of the pore collapse stress (marked by dot) for the case of (a) deionized water saturated chalk, (b) sodium chloride solution saturated chalk, (c) magnesium chloride solution saturated chalk, (d) calcium chloride solution saturated chalk and (e) sodium sulfate solution saturated chalk.

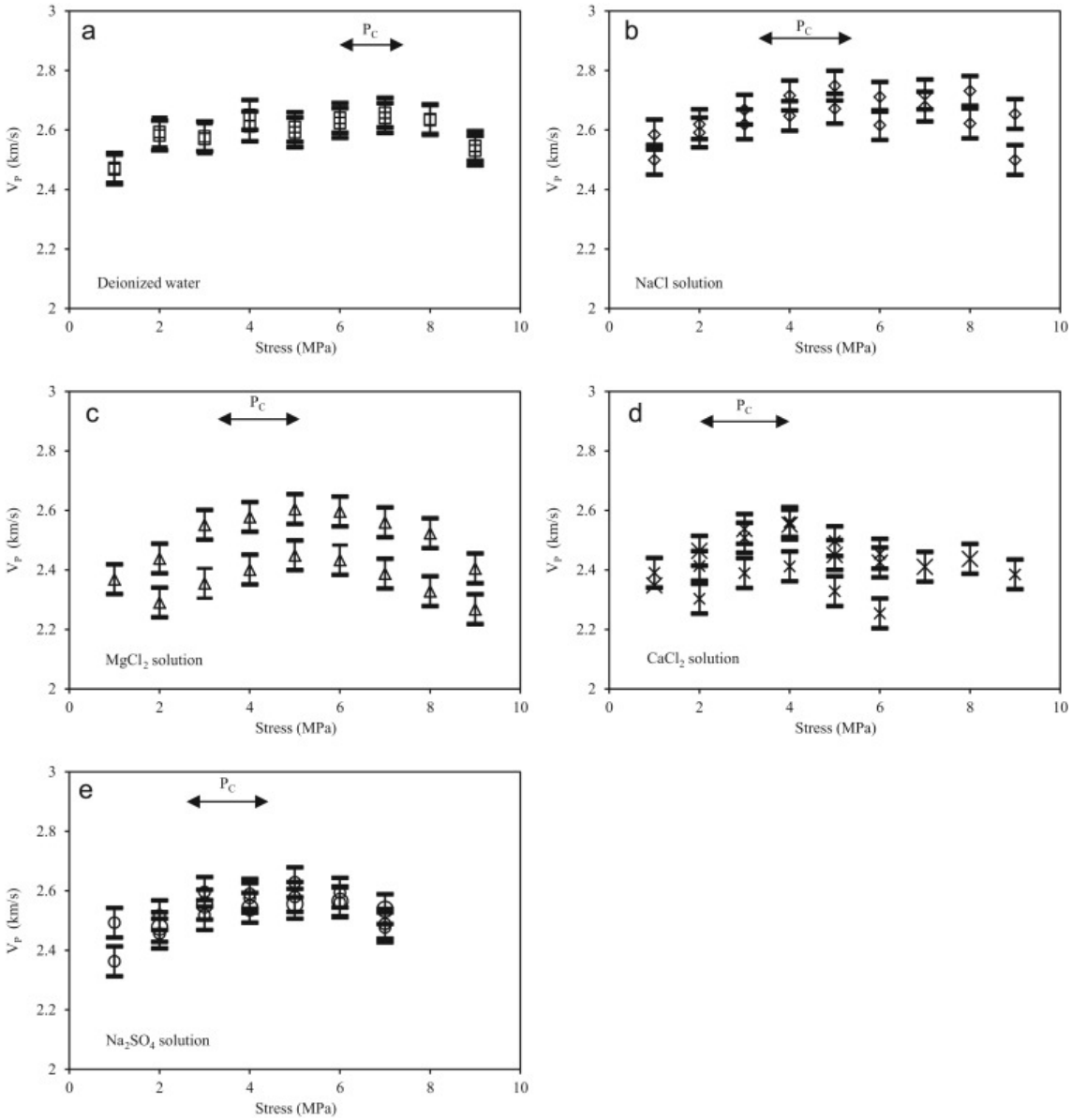

Figure 8.4. Compressional wave velocity vs. axial stress during testing and calculations for all samples arranged in groups of similar pore fluid, a) deionized water, b) sodium chloride solution, c) magnesium chloride solution, d) calcium chloride solution and e) sodium sulphate solution plugs. The average pore collapse stress is marked with arrows in each diagram as shown in Figure 8.3 (Katika et al., II).

Figure 8.5 gives an overview of the pore collapse stresses of all the samples. We find that samples saturated with deionized water withstand higher stresses before pore collapse. Saturation with sodium chloride brine corresponds to a weaker rock than those saturated with deionized water, but also leads to pore collapse at higher stress levels than saturation with Mg-rich brines. Core plugs saturated with sodium sulfate brine experience pore collapse at smaller stresses than of those saturated with magnesium

chloride solution. If we use the average value of the stress when pore collapse occurred, the three samples saturated with calcium chloride brine are the weakest of all.

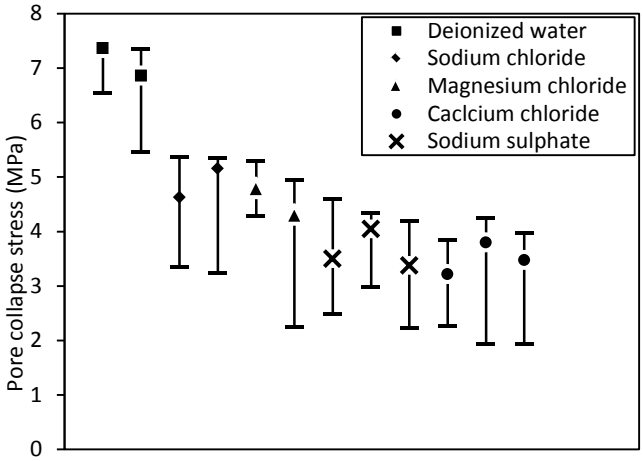

Figure 8.5. The corresponding pore collapse stress when different fluids are used for the saturation of chalk. Pore collapse has lower average value when calcium chloride solution is used for the sautation and the highest value when the chalk is saturated with deionized water (Katika et al., II).

Chalks saturated with divalent ions are more sensitive to rock mechanical tests and they are weaker supporting previous observations reported by Heggheim et al., (2005), Kornes et al., (2008), Madland et al., (2011), Megawati et al., (2013) and Nermoen et al., (2015). Nermoen et al., (2015), investigated the mechanical properties of Liege chalk and observed a weaker rock when the pore space was occupied with sodium sulfate brines than with sodium or magnesium chloride brines. Their model about the enhancement of the electrostatic stresses on the surface of chalk due to the presence of divalent ions comes in agreement with the results in the present study. Risnes et al., (2003), investigated the mechanical properties of quarry chalks from Lixhe near Liege in Belgium and Roerdal near Aalborg in Denmark. These types of chalk have similar properties with chalk from Stevns, used in the present study, with respect to porosity, permeability and carbonate content. Saturation with high salinity sodium chloride brine, resulted in higher moduli and yield stress than saturation with calcium chloride brine. Their results come in agreement with the results in the present study for chalk saturated with brines containing similar types of ions.

8.3 The effect of divalent ions on the T_2 distribution of chalk

The T_2 spectra for each case of saturation were obtained and averaged so as to illustrate the effect of the deionized water and each ion (Na^{1+}, Mg^{2+}, Ca^{2+} and SO_4^{2-}) on wackestone chalk from Stevns Klint (Figure 7.3). The NMR experiments were conducted prior to the mechanical testing. Hence, we obtained the T_2 distribution for three core plugs in each case of saturation which were averaged in Figure 7.3. We observe that chalk saturated with Mg-rich brines results in faster relaxation of the protons than chalk saturated with Ca and SO_4-rich brines. Saturation of carbonates with Mg^{2+} leads to precipitation. As observed in Table 7.1 (MA-samples), the surface-to-volume ratio increases in all cases after the saturation with Mg-rich brines while it is less affected by the saturation with Ca and SO_4-rich brines. Possibly precipitation of magnesium bearing carbonates remain in the pore space of the chalk and leads to increasing specific surface. Since a similar T_2-shift was not observed for Ca and SO_4 ions in brines, these observations indicate that although Mg-carbonates precipitate in the pore space, it cannot be the significant mechanism behind the weakening effect of brines with divalent ions.

9 Third research objective - Katika et al., III

Low field NMR spectrometry of chalk and argillaceous sandstones: rock - fluid affinity assessed from T_1/T_2 ratio

The T_1/T_2 ratio can illustrate the wettability of complex systems; such as rocks with bimodal pore size distributions and two fluids present in the pore space. Two data points are required: one when the water is saturating as a single fluid and another where both oil and water are present in a formation.

9.1 T_2 measurements of the bulk fluids

The T_2 distributions of the bulk salt water (brine) and oil are shown in Figure 9.1a and b, respectively. The crude oil is a mixture of different chemical compounds that relax at different times; hence, the broad T_2 spectrum in Figure 9.1b (Rueslåtten et al., 1994).

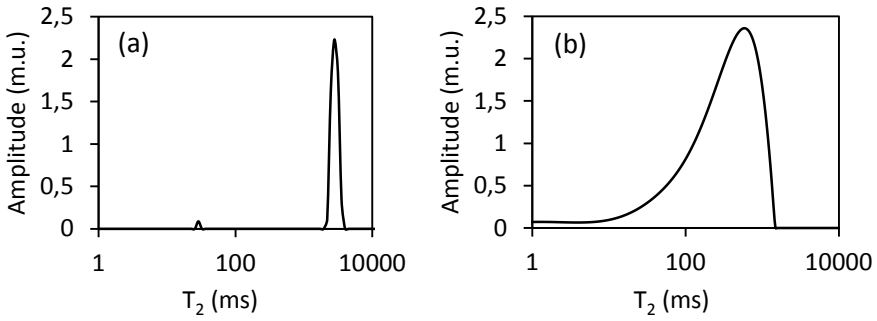

Figure 9.1. The T_2 distribution of the (a) bulk water and (b) bulk oil (Katika et al., III).

9.2 Bulk and surface transverse relaxation

Figure 9.2 presents the T_2 distributions for each lithology for each saturation state. The NMR porosity of the fully water saturated plugs was derived from the T_2 distributions (Coates et al., 1999). The NMR porosity values are practically similar to the porosity measured with helium expansion on dry rocks (Table 6.2).

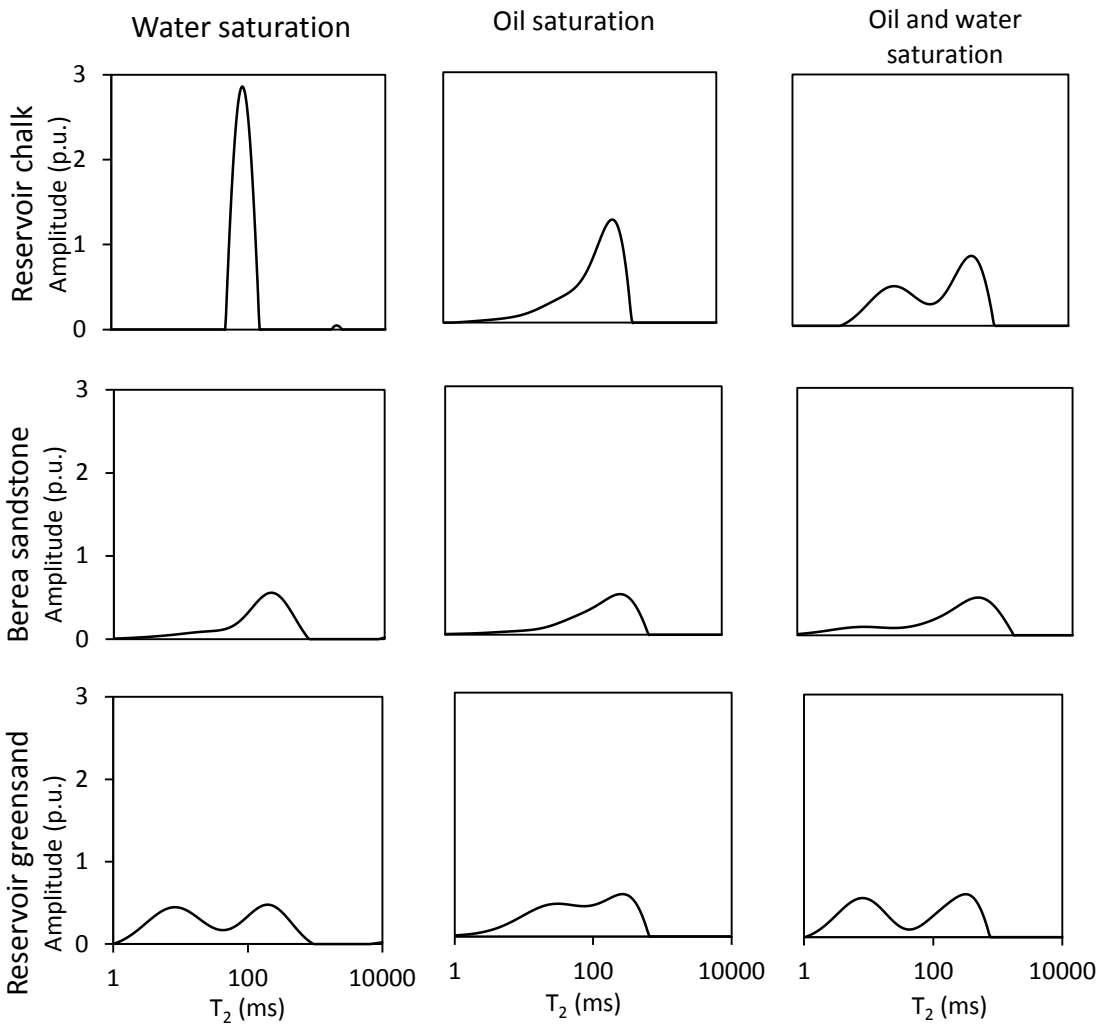

Figure 9.2. The T_2 distributions of the chalk from the Gorm field (first row), Berea sandstone (second row) and greensand from the Solsort field (third row). The first column consists of rocks saturated with water, the second column of rocks saturated with oil and the third column of rocks saturated with oil and water at irreducible water saturation (Katika et al., III).

The T_2 distributions of the water saturated chalk, Berea sandstone and greensand resemble the MICP throat size distributions in Figures 6.1, 6.4 and 6.5 respectively. The similarity of the two distributions has been illustrated in previous studies for porous rocks, including water saturated Bentheimer sandstone, Berea sandstone, chalk and Texas Cream limestone (Marschall et al., 1995; Liaw et al., 1996). The slow bulk relaxation of the free water seems to have no effect on the T_2 distribution of the water saturated rock, indicating that the fluid adsorbs on the surface and the surface relaxation dominates the transverse relaxation.

The T_2 distribution of the oil saturated chalk and Berea sandstone resembles the T_2 spectrum of the bulk oil and does not reflect the pore size distribution of each lithology. The bulk relaxation of the oil dominates the transverse relaxation; and equation (1) no longer describes the total relaxation. This indicates that the fluid, in this case the oil, does not adsorb on the surface of the minerals of chalk and Berea sandstone and therefore, there is no solid-fluid interaction. This observation is in accordance with previous studies which illustrate that the T_2 distribution is a reflection of the pore size distribution only in oil wet rocks (Guan et al., 2002; Fleury and Deflandre, 2003). In Figure 9.2, the T_2 distribution of the oil saturated greensand does not reflect only the bulk relaxation of the free oil but a solid-fluid interaction is also indicated since a second peak at lower relaxation times is present. The T_2 spectrum of the oil saturated greensand is thus the result of both surface and bulk relaxation in the pore space. It is worth mentioning that an investigation conducted by Cuiec, 1987, on chloritic greensands from the North Sea, indicated that chlorite is preferably oil-wet (cited in Barclay & Worden, 2000).

The T_2 distribution of the oil and water saturated chalk, Berea sandstone and greensand has two peaks; the left peak probably is the result of solid-bound water interaction, whereas the right peak resembles the bulk relaxation of the free oil. This observation is in accordance with Talabi and Blunt, (2010), and Guan et al., (2002). The water interacts with the surface of the mineral while the oil relaxes according to the bulk relaxation suggesting that there is no interaction of this fluid with the pore walls.

9.3 Microscopic field gradients and restricted diffusion

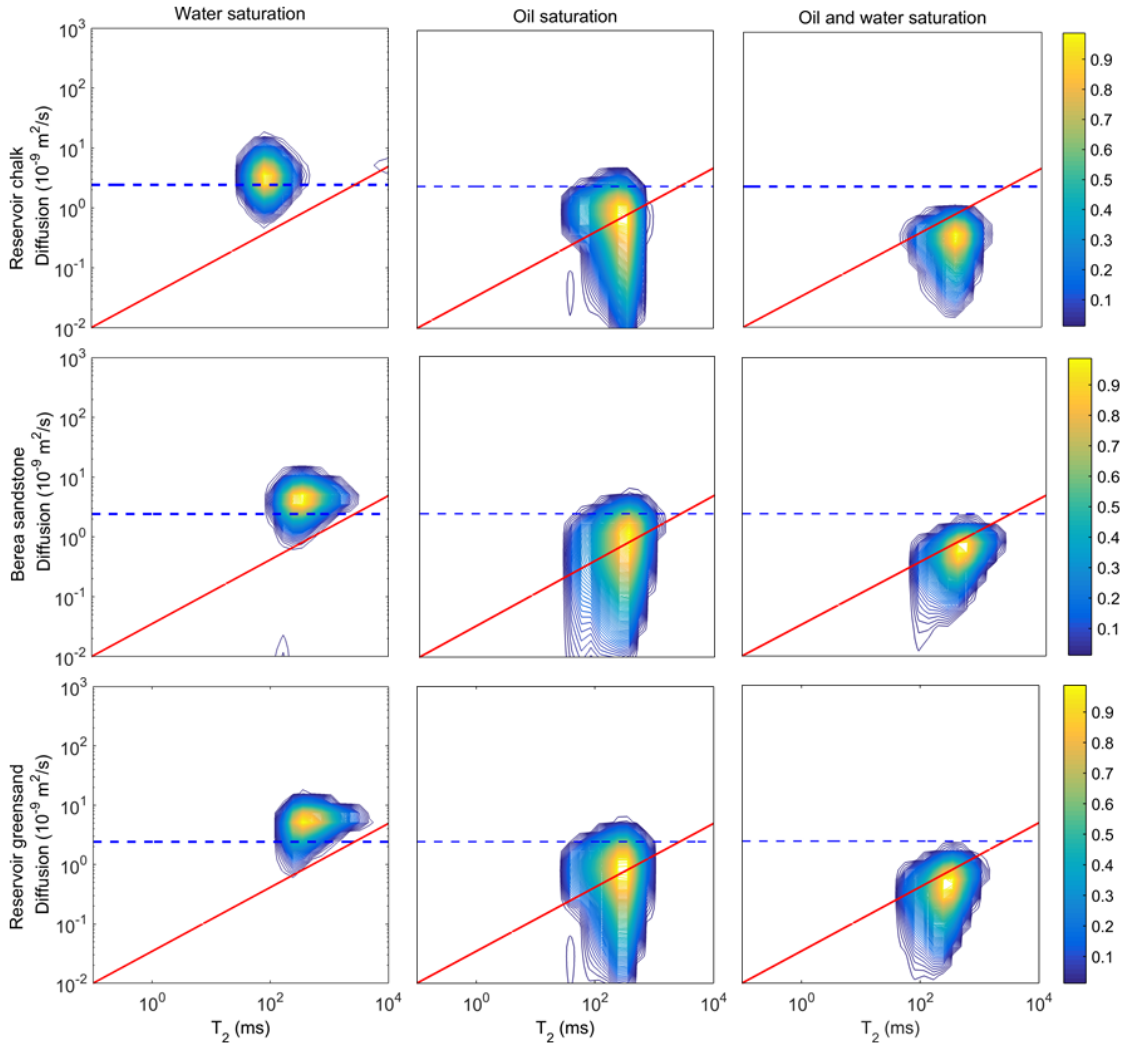

Figure 9.3. The *D*-T_2 maps of chalk from the Gorm Field, Berea sandstone and greensand from the Solsort field. The first column represents rocks saturated with water, the second column rocks saturated with oil and the third rocks saturated with oil and water at irreducible water saturation. The horizontal dashed line indicates the molecular diffusion coefficient of water, whereas the inclined dashed line shows the correlation between the average diffusion coefficient and average relaxation times of oil according to Hurlimann et al., 2002 (Katika et al., III).

Figure 9.3 presents the *D*-T_2 maps for all the plugs. In the *D*-T_2 maps lines have been drawn that illustrate the *D*-T_2 response of the bulk water and oil (Hurlimann et al., 2003). The fluid self-diffusivity coefficient was measured with the PGSE pulse sequence prior to the experiments; $2.58 \cdot 10^{-10}$ m^2/s for the water and $2.42 \cdot 10^{-9}$ m^2/s for the oil at 40^{o}C. The horizontal line in each map indicates the molecular self-diffusion coefficient of water; the inclined line indicates diffusion-relaxation correlations for the

crude oil used in this study based on the density and viscosity in Table 4.2 (Lo et al., 2002).

The correlation of T_2 and self-diffusivity coefficient for the fluid in the pore space of the water saturated chalk matches the water line (horizontal line in Figure 9.3) of the map in the first column of Figure 9.3. For the case of the water saturated Berea sandstone and greensand, the D-T_2 correlation of the fluid in the rock shows a higher self-diffusivity coefficient than the water indicating the presence of internal field gradients due to paramagnetic minerals (Hurlimann et al., 2004; Flaum et al., 2005).

The D-T_2 correlation of chalk, Berea sandstone and greensand fully saturated with oil matches the free oil line (inclined line in Figure 7). Effects of the internal field gradients are not expected in the oil saturated chalk and Berea sandstone, since there is no oil-solid interaction. In the case of greensand the single peak indicates that effect of diffusion of oil probably is only seen for the large pores.

For the rocks that have both oil and water in their pore space we might expect to see two different regions; one matching the water line and one matching the oil line due to the difference in the self-diffusion coefficient of the two fluids. But, we observed only values below the horizontal "water" line indicating the restricted diffusion. This is in accordance to previous studies that illustrated that the water is unable to illustrate the effects of the macroscopic field gradients unless the amount of water present in the rocks is high (Hurlimann et al., 2004; Flaum et al., 2005). All samples show values close to, but bellow the line representing the free oil. This indicates that the presence of water to some degree restricts the diffusion of oil.

9.4 Wettability determination from T_1/T_2

Figure 9.4 presents the T_1-T_2 maps for all the plugs. We divided each T_1-T_2 map in two regions; one for relaxation times lower than 50 ms and the other one for higher values. For each region, the T_1/T_2 ratio was calculated at the point of highest intensity in the map (light yellow colour). For example, in the case of water saturated chalk we only

observe one region for higher values, whereas, when the same rock has both oil and water, two regions are shown in the same map. Table 9.1 summarizes all the results.

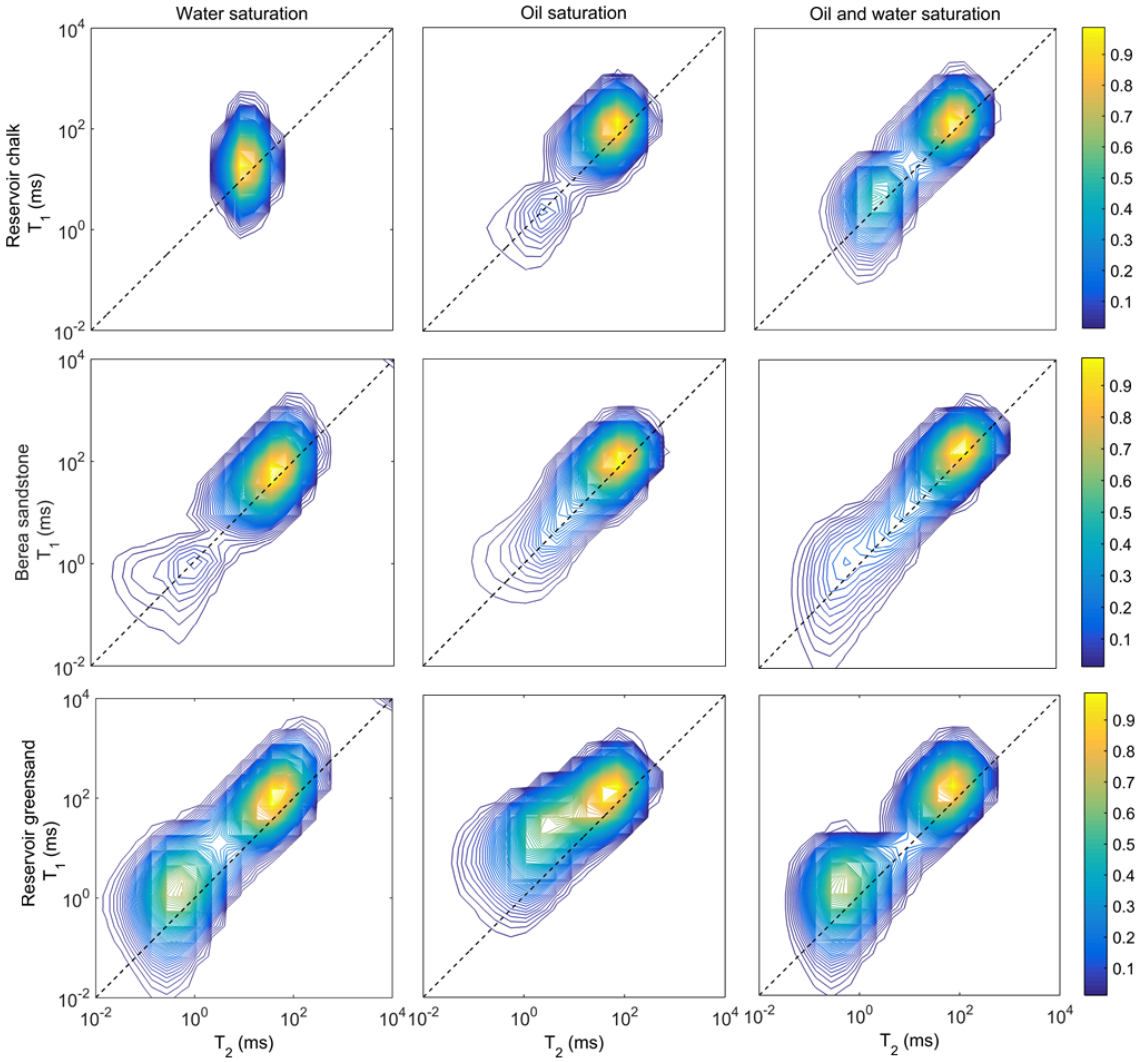

Figure 9.4. ***T_1-T_2*** **maps of chalk from the Gorm field, Berea sandstone and greensand from the Solsort field. The first column represents rocks saturated with water, the second column rocks saturated with oil and the third one rocks saturated with oil and water at irreducible water saturation (Katika et al., III).**

In the case of chalk, the T_1/T_2 ratio is higher when there is water instead of oil present in the pore space. In the case of both oil and water saturated chalk, the left peak has higher T_1/T_2, representing the strong attraction of the water to the surface. The T_1/T_2 ratio is higher when water comes in contact with the surface of the mineral than when oil wets the surface. The increase in the ratio indicates the strong water-chalk affinity.

Table 9.1. The T_1/T_2 ratio of the rocks from the 2D maps T_1-T_2 at Figure 9.4.

Sample	Lithology	Saturation	T_2 < 50 ms T_1/T_2	T_2 > 50 ms T_1/T_2
N-3X-T1	Chalk (Gorm field)	Water	-	2.0
N-3X-T2		Oil	1.0	1.2
N-3X-T3		Oil and water	2.3	1.4
BS-T1	Berea sandstone	Water	-	1.2
BS-T2		Oil	1.1	1.1
BS-T3		Oil and water	1.4	1.1
GSD-T1	Greensand (Solsort field)	Water	2.0	2.2
GSD-T2		Oil	3.8	1.2
GSD-T3		Oil and water	1.9	1.6

In the case of Berea sandstone the T_1/T_2 ratio is similar in both regions when there is either water or oil present in the pore space. In the case of both oil and water saturated rock, the first peak has relatively higher T_1/T_2; but the negligible differences could be interpreted as a neutral response to both water and oil.

In the case of greensand the T_1/T_2 ratio of the fast relaxing components (small pores) is higher when there is oil instead of water present in the pore space. On the other hand, the slow relaxing components (big pores) have a higher ratio when in contact with water than with oil. Of the two minerals that dominate the mineralogy of greensand, chlorite occupies the small pores and shows high oil attraction compared to quartz. This could be an indication of the mixed wettability of the rock.

9.5 Fluid substitution

Figure 9.5a illustrates the bulk moduli of the frame, K_f , of the water saturated rocks compared to the K_f of the rocks saturated with both oil and water where the effective bulk moduli of the mixed fluid was determined using the Voigt bound. Figure 9.5b illustrates the K_f of the oil saturated rocks compared to the K_f of the rocks saturated with both oil and water as the effective bulk moduli of the mixed fluid was determined using the Reuss bound. In both figures, all K_f were subtracted from the bulk moduli of the dry rock, K_{dry}, to minimize the visual effects of porosity differences among the samples.

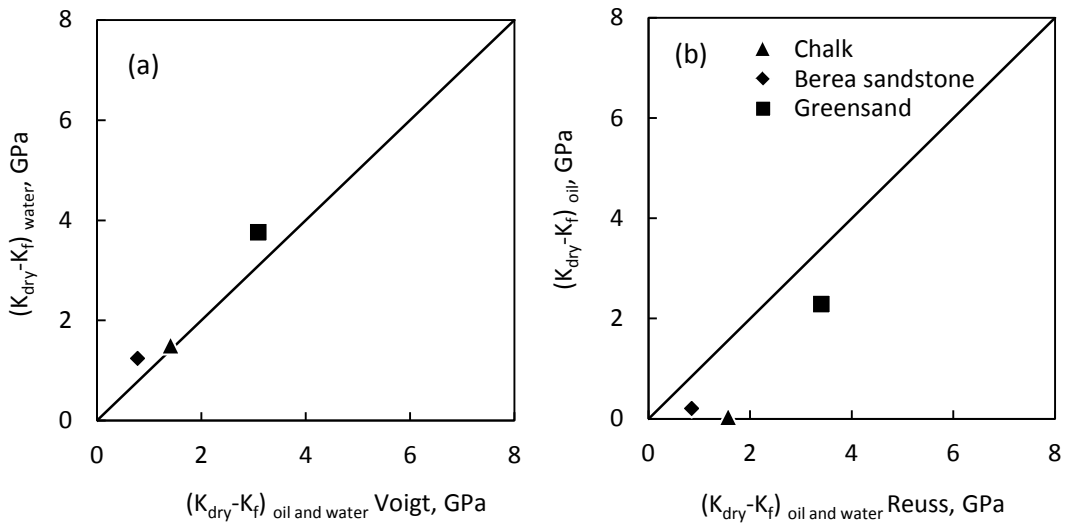

Figure 9.5 (a) The frame bulk modulus K_f of the water saturated rocks vs. the K_f of the oil and water saturated rocks at irreducible water saturation where the Voigt bound defines the effective bulk modulus of the fluids in the pore space. (b) The K_f of the oil saturated rocks vs. the K_f of the oil and water saturated rocks at irreducible water saturation where the Reuss bound defines the effective bulk modulus of the fluids in the pore space. All K_f are subtracted from the K_{dry} of the samples in order to focus on fluid effects (Katika et al., III).

From the bulk moduli of the oil and water saturated chalk illustrated in Figure 9.5a we observe that the K_f calculated at the Voigt bound is similar to the K_f of the water saturated chalk and that using the Reuss bound for chalk leads to a huge overestimation of the frame stiffness (Figure 9.5b). This indicates that for the case of chalk in the presence of both oil and water in the pore space, water is the fluid supporting the frame. For the two sandstones, using the Voigt bound leads to lower frame stiffness (Figure 9.5a) indicating that the fluid mixture is softer than the Voigt bound. On the other hand, using the Reuss bound leads to high prediction of the frame stiffness (Figure 9.5a). These observations support the results for NMR, indicating the chalk is water wet whereas the two sandstones are intermediate or respectively mixed wet.

10 Fourth research objective - Katika et al., IV

Quantification of small amounts of oil in water

During core flooding experiments, the oil-bearing core plugs are subjected to water injection. As a result, both oil and water are produced from the cores and typically collected in vials. A typical core flooding equipment (Figure 10.1a) consists of : i) a piston displacement pump with fluid accumulators to force fluid into a core plug, ii) a test unit (the core plug inside a heated and pressurized core holder, to simulate oil reservoir conditions) and iii) a production unit, where the injected fluids are collected.

Collection of the produced fluids (effluents) may be carried out by using a two or three-phase separator (Gupta et al., 2015). However, in this case, monitoring e.g. the presence of an active EOR component or changing pH and salinity is difficult (Stoll et al., 2011). If continuous chemical analysis is required, the produced oil and water should be sampled in a fraction collector containing series of vials (Figure 10.1b). Each vial collects a given amount of effluent during time and is exchanged for a new vial automatically.

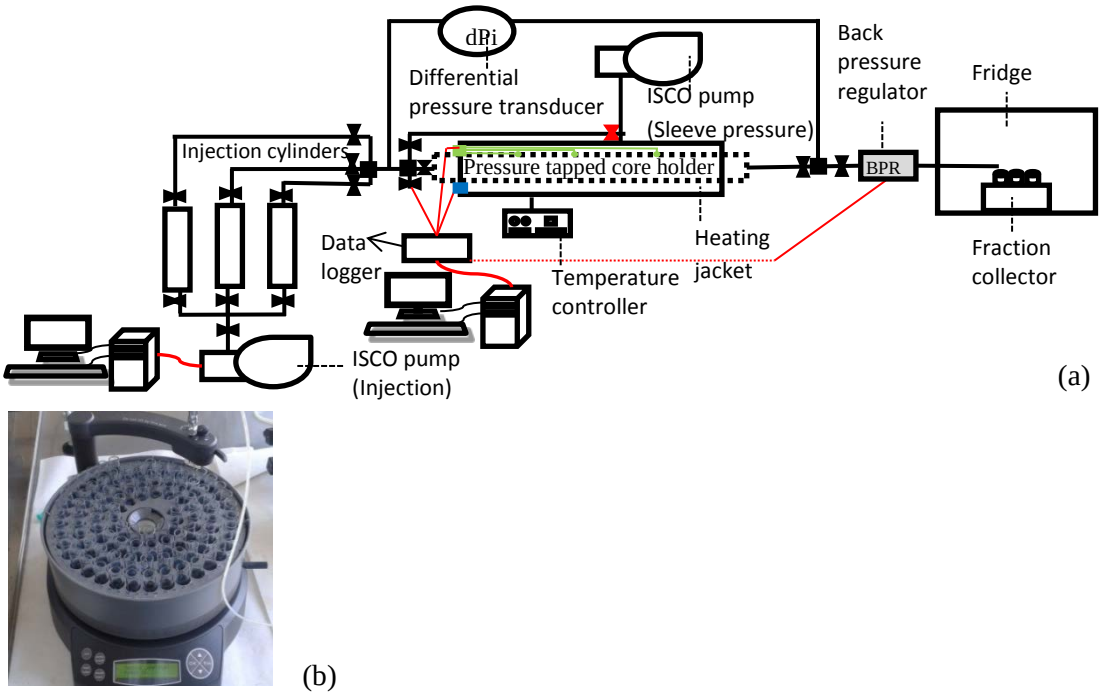

Figure 10.1. (a) Core flooding apparatus and (b) fraction collector with vials (Katika et al., IV).

In a typical core flooding experiment, the amount of oil in the produced fluid gradually decreases after water breakthrough. The recovered oil is distributed among several vials, and some vials may contain only few microliters of oil. Due to capillary phenomena, the interface of oil to air is concave and the interface of oil to water is convex (Figure 10.2a). The opaqueness of the oil will thus create an illusion of more oil within the sample than the actual volume. This causes a systematic error in visual measurement of the oil. The recovered oil may also be disconnected from the continuous oil phase and be attached as film or droplets to the vial walls or form drops in the water (Figure 10.2b) (Tang and Morrow, 1992). Quantification of this dispersed oil cannot be achieved simply by visual observations or weight-volume measurements.

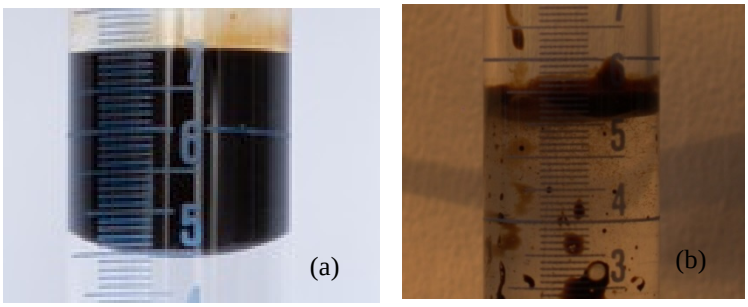

Figure 10.2. (a) The curvature of oil menisci within the vials with 200 microliter of oil and (b) dispersed oil on the walls of the vial (Katika et al., IV).

In the present study, the determination of the produced oil by the four different methods is compared. The simplest method is based on directly reading high-definition photographs of the vials containing oil and water. The three other methods are based respectively on ultraviolet/visible spectroscopy, low field nuclear magnetic resonance spectrometry (NMR), and liquid scintillation counting (LSC). For each method the range of applicability, the accuracy and the time resources involved are evaluated.

10.1 Analysis of samples

Figures 10.3, 10.4, 10.5 and 10.6 show the accuracy of each technique to determine the oil volume. Figure 10.7 shows the accuracy of the NMR spectrometry to detect the water volume in predetermined oil and water samples.

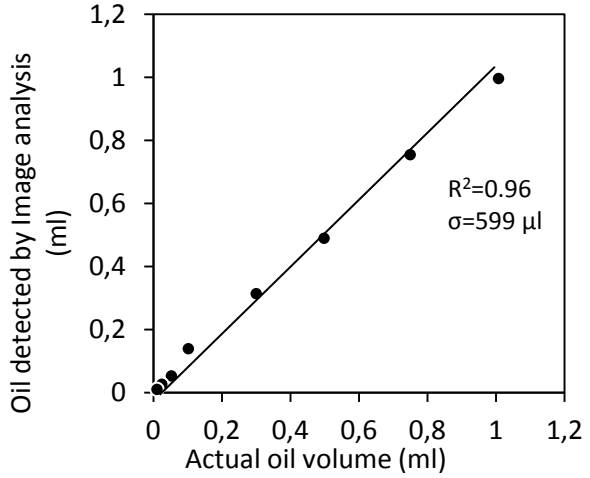

Figure 10.3. The detected volume of oil plotted against the actual oil volume using the Image analysis technique (Katika et al., IV).

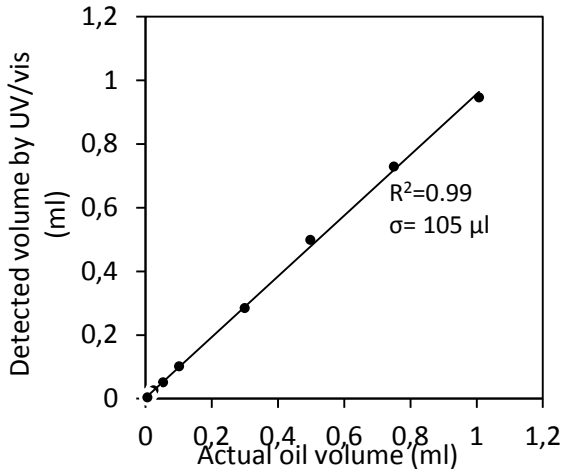

Figure 10.4. The detected volume of oil plotted against the actual oil volume using the UV/visible spectroscopy (Katika et al., IV).

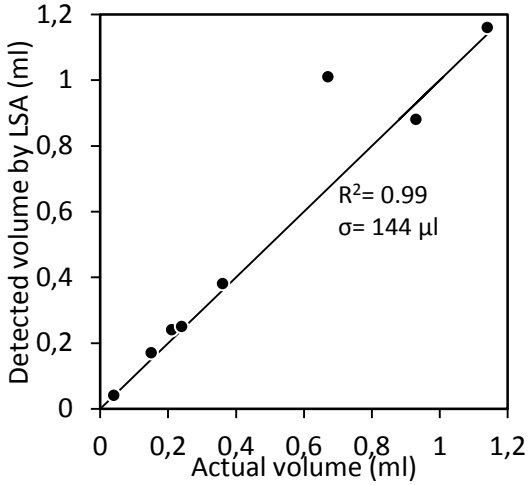

Figure 10.5. The detected volume of oil plotted against the actual oil volume using the liquid scintillation analysis (Katika et al., IV).

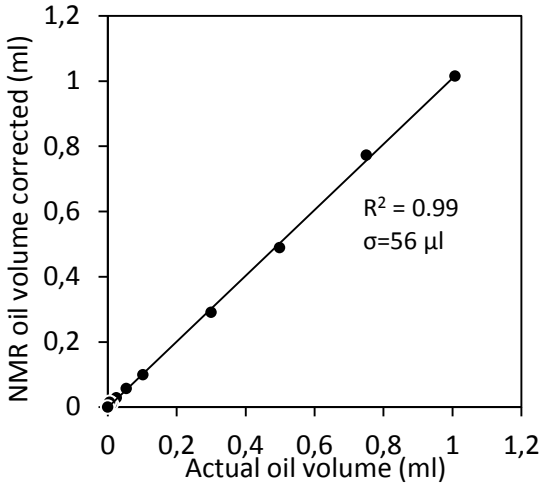

Figure 10.6. The volume detected and plotted against the actual oil volume using low field NMR spectrometry (Katika et al., IV).

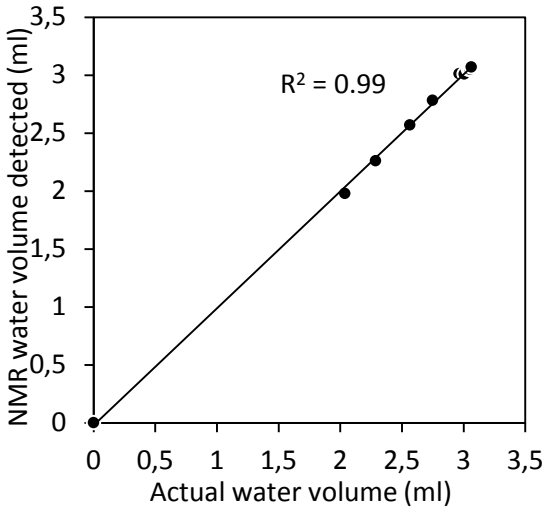

Figure 10.7. The water volume detected from the low field NMR spectrometry (Katika et al., IV).

We were able to obtain a good correlation of the amount of oil added in the glass containers and the amount of oil detected from all four techniques as reflected in high correlation coefficient (R) and low standard deviation (σ) for the analysis of the samples (n) (Table 10.1).

Low field NMR spectrometry and UV/visible spectroscopy are able to detect the oil of the samples within a wide range of oil volumes; from a few microliters to several millilitres. Low field NMR spectrometry was shown to be the most precise in respect to quantification of the oil fractions, but UV/visible spectroscopy produced almost similar

accuracy throughout the measurements, as illustrated by correlation coefficients and standard deviations (Table 10.1). But UV/visible spectroscopy is a user dependent technique that requires manual operation to add toluene to the samples and the use of standard curves which might introduce errors to the results. The standard curves for this technique must be produced with the same oil sample that is going to be analyzed. If the oil volume is higher than 0.2 ml the sample should be diluted several times and an error from the extensive manual dilution might be introduced. Finally, low field NMR spectrometry provides an accurate determination of the water fraction within each sample, giving the opportunity to quantify the amount and the type of fluids within each sample. A drawback of the NMR method is that the entire volume of the fluid should be within 5 cm height. Similarly to the two abovementioned techniques, liquid scintillation analysis resulted in a high correlation coefficient and low residual in the wide range of oil samples (Table 10.1).

Table 10.1. The correlation coefficient (*R*) and the standard deviation (σ) of the samples (*n*) analyzed in each method (Katika et al., IV).

Method	n	R^2	σ (μl)
Image analysis	10	0.96	599
UV/visible spectroscopy	10	0.99	105
Liquid scintilation analysis	8	0.99	144
Low field NMR	10	0.99	56

11 Conclusions

Laboratory experiments and mineralogical investigation conducted on core plugs saturated with different fluids evaluated the effect of salinity and specific ions (Na^{1+}, Mg^{2+}, Ca^{2+} and SO_4^{2-}) on the surface-to-volume ratio of chalk samples from Stevns Klint with two different textures.

- Low field NMR spectrometry was successfully used to identify changes in the surface-to-volume ratio of chalk after the saturation with brines containing divalent ions. The same technique was used successfully to detect the precipitation reactions that occurred among the magnesium, calcium and sulfate ions and carbonates.
- The T_2 relaxation rate of chalk was significantly affected by changes in the surface-to-volume ratio when the surface relaxivity was assumed constant. Chalk saturated with Mg-rich brines resulted in a shift to low T_2, indicating precipitation within the pore space of the medium that increases the specific surface of the pore space. The reaction between calcium and sulfate ions and carbonates led to an increase in T_2, probably resulting from coating of the calcite crystals of the mudstone chalk and the resulting reduction of the specific surface of the pore space. Two different blocks of chalk with different texture illustrate how T_2 relaxation time varies as a result of different specific surface of the pore space.

The effect of pore water composition on the elasticity and strength of chalk plugs was evaluated by mechanical testing and low field NMR spectrometry.

- From rock mechanical testing, it was observed that divalent ions in high concentration affect the elasticity of chalk. High salinity and especially potential determining ions (Mg^{2+}, Ca^{2+} and SO_4^{2-}) soften the rock and promote pore collapse at lower stresses as observed by rock mechanical tests.
- T_2 distributions indicate the precipitation of magnesium carbonates in the pore space in samples with Mg-rich brines, but because the distributions do not show something similar for chalk saturated with brine rich in Ca^{2+} and SO_4^{2-} ions, the precipitation cannot in general explain the water-weakening of chalk.

Low field NMR and ultrasonic velocity measurements were done on chalk from the Gorm field, Berea sandstone and greensand from the Solsort field at three different saturation states; water, oil and oil and water at irreducible water saturation.

- The pore fluid of the reservoir rock relaxes as a free fluid or due to the solid-fluid interaction in the porous medium. Surface relaxation of a pore fluid indicates solid-fluid affinity whereas bulk relaxation indicates the opposite.
- The T_1/T_2 ratio was used as a mechanism to quantify the fluid-solid affinity in reservoir rocks. The T_1/T_2 ratio illustrates the strength with which a fluid adsorbs on a solid; the higher the adsorption strength the higher the ratio. The fluid wetting the surface of a mineral has higher ratio than other fluids present in the pore space.
- D-T_2 maps illustrate the presence of microscopic field gradients and restricted diffusion in the pore space of reservoir rocks.
- The fluid distribution obtained from the T_1/T_2 ratio can be applied when estimating the fluid moduli in rocks, bearing two fluids, by mixing compounds according to Voigt average in the water wet case, the Reuss average in the oil wet case and a Hill average in the intermediate or mixed wet case. This is relevant for Gassmann's fluid substitution in elasticity studies for core and log analysis.

The determination of the produced oil in effluents was compared by four different methods.

- Low field NMR spectrometry was shown to be the most precise technique in respect to accurate quantification of the oil fractions.
- Low field NMR spectrometry provides an accurate determination of the water fraction within each sample, giving the opportunity to quantify the amount and the type of fluids within each sample.
- The water and oil face do not have to be separated when determining small amounts of oil in water with low field NMR spectrometry.

References

Alam, M.M., 2011, Rock physical aspects of CO2 injection in chalk, Ph.D. thesis, Technical University of Denmark (DTU), Kgs. Lyngby, Denmark.

Ali, A.Y., Salah Hamad, A.S., Abdulaziz, A.K., and Mohammed Saleh, A.J., 2011, Laboratory Investigation of the Impact of Injection Water Salinity and Ionic Content on Oil Recovery From Carbonate Reservoirs, *SPE Reservoir Evaluation & Engineering*.

Allsopp, K., Wright, I., Lastockin, D., Mirotchnik, K., and Kantzas, A., 2001, Determination of Oil and Water Compositions of Oil/Water Emulsions Using Low Field NMR Relaxometry. *Petroleum Society of Canada*, **40**(7), 58-61.

Al-Mahrooqi, S., Grattoni, C.A., Moss, A.K. and Jing, X.D., 2003, An investigation of the effect of wettability on NMR characteristics of sandstone rock and fluid systems, *Petroleum Science and Engineering*, **39**, 389– 398.

Andersen, P.Ø., Evje, S., Madland, M.V., and Hiorth, A., 2012, A geochemical model for interpretation of chalk core flooding experiments, *Chemical Engineering Science*, **84**, 218-241.

Andreassen, K.A. and Fabricius, I. L., 2010, Biot critical frequency applied to description of failure and yield of highly porous chalk with different pore fluids, *Geophysics*, **75**(6), E205-E213.

Austad, T., Strand, S., Høgnesen, E.J. and Zhang, P., 2005, Seawater as IOR Fluid in Fractured Chalk, SPE International Symposium on Oilfield Chemistry, *Society of Petroleum Engineers Inc.*, The Woodlands, Texas.

Austad, T., Strand, S., Madland, M.V., Puntervold, T., and Korsnes, R.I., 2008, Seawater in chalk: An EOR and compaction fluid, *SPE Reservoir Evaluation and Engineering*, **11**(4), 648-654.

Bader, M.S.H., 2006, Sulfate scale problems in oil fields water injection operations, Desalination, **201**(1-3), 100-105.

Berg, S., Cense, A.W., Jansen, E., and Bakker, K., 2010, Direct experimental evidence of wettability modification by low salinity, *Petrophysics*, **51**(5), 314.

Biot, M.A., 1941, General theory of three-dimensional consolidation, *Journal of applied physics*, **12**(2), 155-164.

Borgia, G.C., Brown, R.J.S. and Fantazzini, P., 1991, Nuclear magnetic resonance relaxivity and surface-to-volume ratio in porous media with a wide distribution of pore sizes, *Applied Physics*, **79**,3656-3664.

Brunauer, S., Emmett, P.H. and Teller, E., 1938, Adsorption of gases in multimolecular layers, *American Chemical Society*, **60**(2), 309-319.

Churcher, P.L., 1991, Rock properties of Berea sandstone, Baker dolomite, and Indiana limestone, SPE International Symposium on Oilfield Chemistry, Anaheim, 431–466

Coates, G. R., Xiao, L. and Prammer, M. G., 1999, *NMR logging: principles and applications*, s.l.:Gulf Professional Publishing.

Cook, C.C. and Jewell, S., 1996, Simulation of a North Sea field experiencing significant compaction drive, *SPE Reservoir Engineering*, 48-53.

D'Agostino, C., Mitchell, J., Mantle, and Michael D., Gladden, L.F., 2014, Interpretation of NMR Relaxation as a Tool for Characterising the Adsorption Strength of Liquids Inside Porous Materials, *Chemistry European Journal*, **20**(40), 13009-13015.

De Gennaro, V., Delage, P., Priol, G., Collin, F., and Cui, Y.J., 2004, On the Collapse Behavior of Oil Reservoir Chalk, *Géotechnique*, **54**(6), 415-420.

Delage, P., Schroeder, C. and Cui, Y.J., 1996, Subsidence and capillary effects in chalks, Symposium International ISRM, Eurock'96, Turin, 1291-1298.

Diaz, D. C., Breda, E., Minetto, C., & Songhua, C., 1999, Use of NMR Logging for Formation Damage Prevention: Water-Flooding Case Study in Cañadón Seco, San Jorge Basin, SPE-56425-MS.

Dunn, K., Bergman, D.J. & LaTorraca, G.A., 2002, *Nuclear Magnetic Resonance-Petrophysical and Logging Applications.* New York: Handbook of Geophysical Exploration: Seismic Exploration, Pergamon Press.

Evdokimov, I.N., Eliseev, N.Y., & Akhmetov, B.R., 2003a, Assembly of asphaltene molecular aggregates as studied by near-UV/visible spectroscopy: I. Structure of the absorbance spectrum, *Petroleum Science and Engineering*, **37**(3–4), 135-143.

Evdokimov, I.N., Eliseev, N.Y., & Akhmetov, B.R., 2003b, Assembly of asphaltene molecular aggregates as studied by near-UV/visible spectroscopy: II. Concentration dependencies of absorptivities, *Petroleum Science and Engineering*, **37**(3–4), 145-152.

Fabricius, I.L., 2003, How burial diagenesis of chalk sediments controls sonic velocity and porosity, *AAPG bulletin*, **87**, 1755–1778.

Fathi, S.J., Austad, T., & Strand, S., 2010, "Smart Water" as a Wettability Modifier in Chalk: The Effect of Salinity and Ionic Composition, *Energy & fuels*, **24**, 2514-2519.

Flaum, M., Chen, J., & Hirasaki, G. J., 2005, NMR Diffusion Editing for D–T2 Maps: Application to Recognition of Wettability Change, *Petrophysics*, **46**(2), 113-123.

Fleury, M., & Deflandre, F., 2003, Quantitative evaluation of porous media wettability using, *Magnetic Resonance Imaging*, **21**, 385-387.

Gassmann, F., 1951, Uber die Elastizitaet poroeser Medien: Vierteljahresschrift der Naturforschenden Gesellschaft, Zuerich, **96**, 1–23.

Guan, H., Brougham, D., Sorbie, K.S. & Packer, K.J., 2002, Wettability effects in a sandstone reservoir and outcrop cores from NMR relaxation time distributions, *Petroleum Science and Engineering*, **34**, 35–54.

Gupta, R., Glotzbach, R., Hehmeyer, O., 2015, A Novel Field-Representative Enhanced-Oil-Recovery Coreflood Method, *SPE Journal*, Preprint, 21 – 34.

Grombacher, D., Vanorio, T., & Ebert, Y., 2012, Time-lapse acoustic, transport, and NMR measurements to characterize microstructural changes of carbonate rocks during injection of CO2-rich water, *Geophysics*, **77**(3), 169-179.

Heggheim, T., Madland, M.V., Risnes, R., & Austad, T., 2005, A chemical induced enhanced weakening of chalk by seawater, *Petroleum Science and Engineering*, **46**(3), 171-184

Hirasaki, G., Lob, S.W. & Zhangc, Y., 2003, NMR properties of petroleum reservoir fluids, *Magnetic Resonance Imaging*, **21**(3-4), 269–277.

Hirasaki, G., Miller, C. A., & Puerto, M., 2011, Recent Advances in Surfactant EOR, *SPE Journal*, **16**(04), 889-907.

Hiorth, A., Cathles, L., & Madland, M., 2010, The Impact of Pore Water Chemistry on Carbonate Surface Charge and Oil Wettability, *Transport Porous Media*, **85**(1), 1–21.

Hsu, W., Li, X. & Flumerfelt, R.W., 1992, Wettability of Porous Media by NMR Relaxation Methods, Washington, DC, SPE24761.

Huirlimann, M.D., Freedman, R., Venkataramanan, L., Flaum, C., Flaum, M., Hirasaki, G. J., 2003, Diffusion-relaxation distribution functions of sedimentary rocks in different saturation states, *Magnetic Resonance Imaging*, **21** (3-4), 305-310.

Huirlimann, M.D., Venkataramanan, L., Flaum, C., Speier, P., Karmonik, C., Freedman, R., & Heaton, N., 2002, Diffusion-Editing: New Nmr Measurement Of Saturation And Pore Geometry, SPWLA 43rd Annual Logging Symposium, June 2-5.

Hürlimann, M.D., Matteson, A., Massey, J.E., Allen, D.F., Fordham, E.J., Antonsen, F., & Rueslåtten, H.G., 2004, Application of NMR Diffusion Editing as Chlorite Indicator, *Petrophysics*, **45**(5), 414–421.

Jadhunandan, P.P., & Morrow, N.R., 1995, Effect of wettability on waterflood recovery for crude-oil/brine/rock systems, *SPE Reservoir Engineering*, **10**(1), 40-46.

Jiang, T., Rylander, E., Singer, P. M., Lewis, R. E., & Sinclair, S. M., 2013, Integrated Petrophysical Interpretation of Eagle Ford Shale with 1-D and 2-D Nuclear Magnetic Resonance (NMR), *Society of Petrophysicists and Well-Log Analysts*, SPWLA 54th Annual Logging Symposium, 22-26 June, New Orleans, Louisiana.

Keating, K., & Knight, R., 2012, The effect of spatial variation in surface relaxivity on nuclear magnetic resonance relaxation rates, *Geophysics*, **77**(5), E365-E377.

Kleinberg, R. L. & Farooqui, S.A., 1993, T1/T2 Ratio and Frequency Dependence of NMR Relaxation in Porous Sedimentary Rocks, *Colloid and Interface Science*, **158**, 195-198.

Kleinberg, R. L., Kenyon, W.E., Mitra, P.P., 1994, Mechanism of NMR Relaxation of Fluids in Rock, *Magnetic Resonance*, Series A, **108**(2), 206-214.

Korsnes, R.I., Strand, S., Hoff, O., Pedersen, T., Madland, M.V., and Austad T., 2006, Does the chemical interaction between seawater and chalk affect the mechanical properties of chalk, EUROCK 2006, 427-434.

Lager, A., Webb, K.J. , Black, C.J.J., Singleton, M., & Sorbie, K.S., 2008, Low Salinity Oil Recovery - An Experimental Investigation, *Petrophysics*, **49**(1), 28-35.

Latour, L.L., Li, L., & Sotak, C.H., 1993, Improved PFG stimulated-echo method for the measurement of diffusion in inhomogeneous fields, *Magnetic Resonance*, Series B, **101**, 72-77.

Liaw, H.K., Kulkarni, R., Chen, S. & Watson, A. T., 1996, Characterization of fluid distributions in porous media by NMR techniques. *AIChE J., 42.*

Lide, R.D., Milne A. W. G., 1995, Handbook of Data on Common Organic Compounds, Volume II,Compounds F-Z, CRC Press Inc., 1541

Lieser, K.H., 2001, Technical and Industrial Applications of Radionuclides and Nuclear Radiation, in: Nuclear and Radiochemistry: Fundamentals and Applications,Second, Revised Edition, Wiley-VCH Verlag GmbH, Weinheim, Germany, 386.

Madland, M.V., Hiorth, A., Omdal E., Megawati M., Hildebrand-Habel T., Korsnes I. R., Evje S. and Cathles M. L., 2011, Chemical alterations induced by rock-fluid interactions when injecting brines in high porosity chalks, *Transp. Porous Med*, **87**, 679-702.

Madland, M.V., Zimmermann, U., Haser S., Audinot, N.,Gysan P., Korsnes I. R., Schulz, B., Gutzmer, J. and Hiorth A., 2013, Neoformed Dolomite in Flooded Chalk for EOR Processes, 75th EAGE Conference & Exhibition incorporating SPE EUROPEC 2013, London, United Kingdom.

Majid, A.A., Saidian, M., Prasad, M., and Koh, C. A., 2015, Measurement of the Water Droplet Size in Water-in-Oil Emulsions Using low field Nuclear Magnetic Resonance for Gas Hydrate Slurry Application, *Canadian journal of chemistry*, **93**, 1-7.

Majors, P.D., Li, P., and Peters, E. J., 1997, NMR Imaging of Immiscible Displacements in Porous Media, *Society of Petroleum Engineers*, **12**(03), 164-169.

Marschall, D., Gardner, J.S., Mardon, D. and Coates, G.R., 1995, Method for Correlating NMR Relaxometry and Mercury Injection Data, San Francisco, California, USA, SCA-9511.

Mavko, G., Mukerji, T., and Dvorkin, J., 1998. The Rock Physics Handbook: Tools for Seismic Analysis of Porous Media, Cambridge University Press, 329 p.

Mavko, G., Mukerji, T., and Dvorkin J. 2009, The Rock Physics Handbook: Tools for Seismic Analysis of Porous Media, 2nd edn. Cambridge University Press. ISBN 9780521861366.

McDonald, P.J., Korb, J.-P., Mitchell, J., and Monteilhet L., 2005, Surface relaxation and chemical exchange in hydrating cement pastes: A two-dimensional NMR relaxation study, *Phys. Rev*., E 72, 011409

Megawati, M., Madland, M.V., and Hiorth, A., 2012, Probing pore characteristics of deformed chalk by NMR relaxation, *Petroleum Science and Engineering*, **100**, 123–130.

Mitchell, J., Staniland, J., Wilson, A., Howe, A., Clarke, A., Fordham, E. J, and Bouwmeester, R., 2014, Monitoring Chemical EOR Processes, *Society of Petroleum Engineers*, 169155-MS

Mitchell, J., Chandrasekera, T.C., Gladden, L.F., Broche, L.M., and Lurie, D.J., 2013, Exploring Surface Interactions in Catalysts Using Low-Field Nuclear Magnetic Resonance, *Physical Chemistry C*, **117**(34), 17699-17706.

Mortensen, J., Engstrom, F., and Lind, I., 1998, The relation among porosity, permeability, and specific surface of chalk from the Gorm field, Danish North Sea, *SPE Reservoir Evaluation & Engineering*, **1**(3), 245-251.

Morrow, N.R., Tang, G.-Q., Valat, M., and Xie, X., 1998, Prospects of improved oil recovery related to wettability and brine composition, *Petroleum Science and Engineering*, **20**(3-4), 267-276.

Nermoen, A., Korsnes, R. I., Fabricius I.L., and Madland, M.M., 2015, Extending the effective stress relation to incorporate electrostatic effects, in SEG New Orleans Annual Meeting 2015, 3239-3243.

Ozen, A.E., and Sigal, R.F., 2013, T1/T2 NMR Surface Relaxation Ratio for Hydrocarbons and Brines in Contact with Mature Organic-Shale Reservoir Rocks, *Petrophysics*, **54**(1), 11–19.

Pierre, A., Lamarche, J.M., Mercier, R., and Foissy, A., 1990, Calcium as potential determining ion in aqueous calcite suspensions, *Dispersion Science and Technology*, **11**(6), 611-635.

Puntervold, T., and Austad, T., 2007, Injection Of Seawater And Mixtures With Produced Water Into North Sea Chalk Formation: Impact On Wettability, Scale Formation And Rock Mechanics Caused By Fluid-Rock Interaction, SPE 111237.

Puntervold, T., Strand, S., Ellouz, R., and Austad, T., 2015, Modified seawater as a smart EOR fluid in chalk, *Petroleum Science and Engineering*, **133**, 440-443.

Radke, C. J., Kovscek, A. R., and Wong, H., 1992, A Pore-Level Scenario for the Development of Mixed Wettability in Oil Reservoirs, SPE-24880-MS.

Reuss, Z.A.A., 1929, Berechnung der Fliessgrenze von Mischkristallen auf grund der Plastizitätsbedingungen für Einkristalle: Zeitschrift für Angewandte Mathematik und Mechanik, **9**, 49–58.

Risnes, R., Haghighi, H., Korsnes, R.I. and Natvik, O., 2003, Chalk–fluid interactions with glycol and brines, *Tectonophysics*, **370**, 213– 226.

Risnes, R., Madland, M.V., Hole, M. and Kwabiah, N.K., 2005, Water weakening of chalk— Mechanical effects of water–glycol mixtures, *Petroleum Science and Engineering*, **48**(1–2), 21-36.

Rueslåtten, H., Eidesmo, T., Lehne, K.A, and Relling, O.M., 1998, The use of NMR spectroscopy to validate NMR logs from deeply buried reservoir sandstones, Petroleum Science and Engineering, **19**(1–2), 33-43.

Rueslåtten, H., Oren, P.-E., Robin, M., and Rosenberg, E., 1994, A Combined Use of CRYO-SEM and NMR-Spectroscopy for Studying the Distribution of Oil and Brine in Sandstones, SPE/DOE Improved Oil Recovery Symposium, 17-20 April, Tulsa, Oklahoma.

Schoenfelder, W., Gläser H.R., Mitreiter, I., and Stallmach, F., 2008, Two-dimensional NMR relaxometry study of pore space characteristics of carbonate rocks from a Permian aquifer, *Applied Geophysics*, **65**, 21-29.

Seccombe, C.J., Lager, A., Webb, K., Jerauld, G. and Fueng, E., 2008, Improving waterflood recovery: LoSalTM EOR field evaluation, SPE/DOE Imp. Oil Rec. Symposium, Tulsa, Oklahoma.

Settari, A., 2002, Reservoir Compaction, *Society of Petroleum Engineers*, **54**(08), 62-69.

Song, Y.Q., 2010, Recent progress of nuclear magnetic resonance applications in sandstones and carbonates rocks, *Vadoze Zone Journal*, **9**, 828-834.

Strand, S., Høgnesen, E. J., and Austad, T., 2006, Wettability alteration of carbonates-Effects of potential determining ions (Ca2+ and SO42-) and temperature, *Colloids and Surfaces A: Physicochemical and Engineering Aspects*, **275**(1-3), 1-10.

Stoll, W.M., Al Shureqi, H., Finol, J., Al-Harthy Said, A.A., Oyemade Nneamaka S., De Kruijf A., Van Wunnik J., Arkesteijn F., Bouwmeester R., and Faber M.J., 2011, Alkaline/Surfactant/Polymer Flood: From the Laboratory to the Field, *SPE Reservoir Evaluation & Engineering*, **14**(6), 702–712.

Sun, B., Dunn, K.-J., Bilodeau, B.J., Van Dalen, S.C., Stonard, S.W., and Al-Rushaid, A., 2004, Two-Dimensional Nmr Logging And Field Test Results, Society of *Petrophysicists and Well-Log Analysts*.

Talabi, O., and Blunt, M.J., 2010, Pore-scale network simulation of NMR response in two-phase flow, *Petroleum Science and Engineering*, **72** (1-2), 1-9.

Venkataramanan, L., Song, Y. Q. and Hürlimann, M. D., 2002, Solving Fredholm integrals of the first kind with tensor product structure in 2 and 2.5 dimensions, *IEEE Transactions on Signal Processing*, **50**, 1017-1026.

Vledder, P., Fonseca, J. C., Wells, T. Gonzalez, I., and Ligthelm, D., 2010, Low salinity water flooding: Proof of wettability alteration on a field scale, SPE 129564.

Voigt, W., 1910, Lehrbuch der kristallphysik: B.G. Terebner.

Webb, K., and Lager, A., 2008, Comparison of high/low salinity water/oil relative permeability, International Symposium of the Society of Core Analysts, Abu Dhabi, UAE 29 October-2 November, SCA2008-39.

Webb, K.J., Black, C. J.J., and Tjetland, G., 2005, A laboratory study investigating methods for improving oil recovery in carbonates, in International Petroleum Technology Conference, Doha, Qatar.

Weber, D.W., Mitchell, J., McGregor, J., and Gladden, L.F., 2009, Comparing Strengths of Surface Interactions for Reactants and Solvents in Porous Catalysts Using Two-Dimensional NMR Relaxation Correlations, *J. Phys. Chem. C*, **113**, 6610−6615.

Yang, M., 2011, Measurement of Oil in Produced Water, in: Lee, K., Neff J. (Eds.) Produced Water, Springer New York, 74 – 75.

Yousef, A. A., Al-Saleh, S. H., Al-Kaabi, A., and Al-Jawfi, M. S., 2011, Laboratory Investigation of the Impact of Injection-Water Salinity and Ionic Content on Oil Recovery From Carbonate Reservoirs, *SPE Reservoir Evaluation & Engineering*, **14**(5), 578-593.

Zhang, P., Tweheyo, M.T., and Austad T., 2007, Wettability alteration and improved oil recovery by spontaneous imbibition of seawater into chalk: impact of the potential determining ions Ca^{2+}, Mg^{2+}, and SO_4^{2-}, *Colloids Surf. A Physicochem. Eng. Aspects*, **301**, 199–208.

Zielinski, L., Ramamoorthy, R., Minh, C. C., Al Daghar, K. A., Sayed, R. H., and Abdelaal, A. F., 2010, Restricted Diffusion Effects in Saturation Estimates From 2D Diffusion-Relaxation NMR Maps, SPE Annual Technical Conference and Exhibition, 19-22 September, Florence, Italy.

Appendix I – Additional NMR experiments

Additional experiments were set to define the accuracy of the NMR experiments in oil and water samples where the two fluids are not separated. An acoustic shaker was used to mix the oil with the water shown in Table I.1.

Table I.1. Dead oil and synthetic brine samples for NMR oil and water detection experiments.

Sample	Synthetic seawater, ml	Dead oil, ml
a1	2.910	0.000
a2	2.849	0.022
a3	2.820	0.051
a4	2.731	0.096
a5	2.697	0.146
a6	2.663	0.205
a7	2.546	0.241
a8	2.461	0.405
a9	2.250	0.538
a10	1.890	0.797
a11	1.856	0.987
a12	1.010	1.988
a13	0.000	3.170

In initial state both oil and water phases are separated as shown in Figure 10.2a. In the disturbed state, each sample spent 10 minutes in an acoustic shaker when oil started forming oil drops and dispersed on the walls of the glass vials as shown in Figure 10.2b. After spending 30 minutes on an acoustic shaker and a few more minutes of manual shaking the mixture of oil and water appeared to have a uniform light brown colour and therefore the NMR measurements were conducted. Figure I.1 presents the water volumes detected in the NMR experiments against the known volume of oil within the glass vial. In all three cases, initial (separated phases), disturbed and shaken state of the oil and water samples, and the accuracy is above 99%. Similar results are shown in Figure I.2 for the detection of the oil in the same vials. In all cases, the NMR spectrometry was able to quantify the amount of oil and water with high accuracy illustrating that the water and oil phase do not have to be separated for the fluid volume determination.

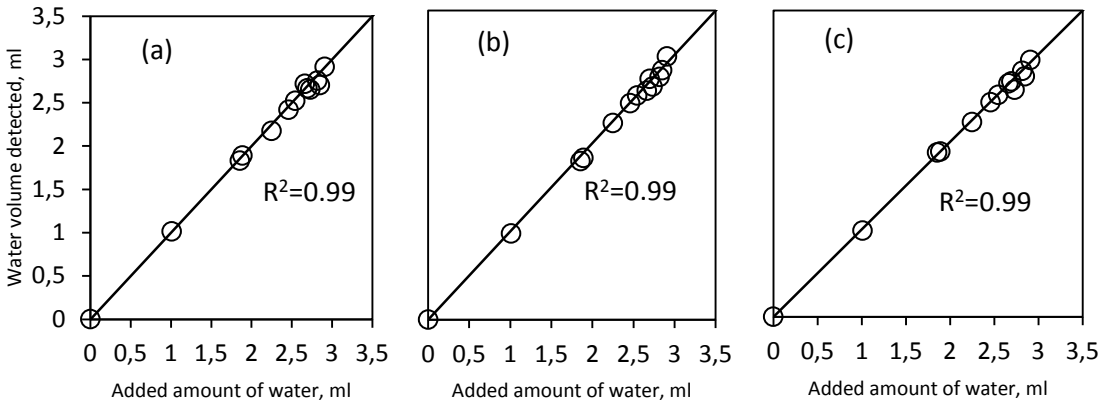

Figure I.1. The water volume detected with NMR in the (a) initial, (b) disturbed and (c) shaken vials of the oil and water.

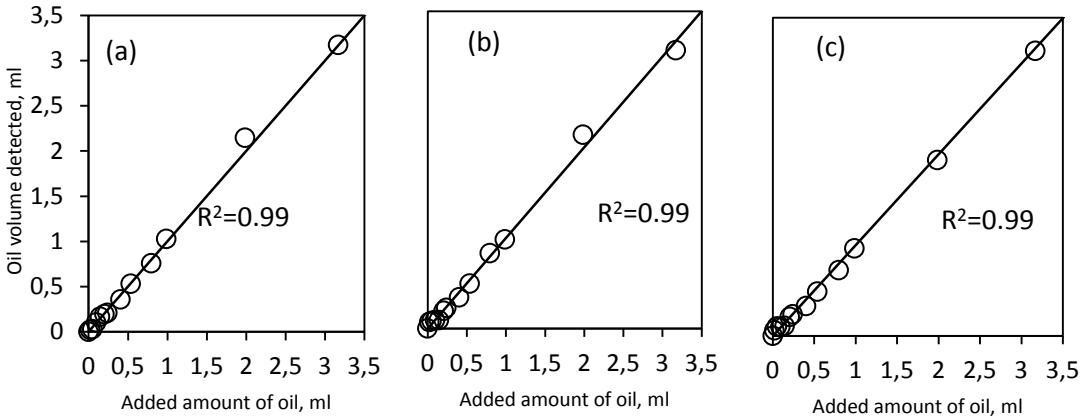

Figure I.2. The oil volume detected with NMR in the (a) initial, (b) disturbed and (c) shaken vials of the oil and water.

Appendix II – Journal manuscripts

Katika et al., I: Changes in Specific Surface as observed by NMR, caused by saturation of Chalk with porewater bearing divalent Ions

Authors	Katika, K., Addassi, M., Alam, M.M., & Fabricius, I.L.
Journal	Diffusion Fundamentals, **22**, 1–14, 2014
Covered in Chapters	7
Status	Published

Katika et al., II: The effect of divalent ions on the elasticity and pore collapse of chalk evaluated from compressional wave velocity and low-field NMR

Authors	Katika, K., Addassi, M., Alam, M.M., & Fabricius, I.L.
Journal	Petroleum Science and Engineering, **136**, 88–99, 2015
Covered in Chapters	8
Status	Published

Katika et al., III: Low field NMR spectrometry of chalk and argillaceous sandstones: rock - fluid affinity assessed from T_1/T_2 ratio

Authors	Katika, K., Saidian, M., Prasad, M., & Fabricius, I.L.
Journal	Petrophysics
Covered in Chapters	9
Status	To be submitted

Katika et al., IV: Comparative analysis of experimental methods for quantification of small amounts of oil in water

Authors	Katika, K., Ahkami, M., Fabricius, I.L., Fosbøl, P.L., Halim, A.Y., Shapiro, A., Thomsen, K., & Xiarchos, I.
Journal	Petroleum Science and Engineering
Covered in Chapters	10
Status	Under review

Appendix III – Additional contributions

New insight into the microtexture of chalks from nmr analysis

Authors	O. Faÿ-Gomord, J. Soete, K. Katika, S. Galaup, B. Caline, F. Descamps, E. Lasseur, I.L. Fabricius, J. Saïag, R. Swennen, S. Vandycke
Submitted	Journal of Marine and Petroleum Geology

Nuclear magnetic resonance and sound velocity measurements of chalk saturated with magnesium rich brine

Authors	Katika, K., Alam, M.M., & Fabricius, I.L.
Submitted	Poromechanics V, 678-684, ASCE, 2013

Nuclear Magnetic Resonance and Elastic Wave Velocity of Chalk Saturated with Brines Containing Divalent Ions

Authors	Katika, K., Alam, M.M., & Fabricius, I.L.
Submitted	75th EAGE Conference & Exhibition incorporating SPE EUROPEC 2013, London, UK, 10-13 June, 2013

Effect of salinity and specific ions on amount of bound water on quartz, calcite and kaolinite, as observed by NMR transverse relaxation time (T_2)

Authors	Alam, M.M., Katika, K., & Fabricius, I. L.
Submitted	76th EAGE Conference & Exhibition 2014, Amsterdam RAI, The Netherlands, 16-19 June, 2014

Electrical tortuosity, Kozeny's factor and cementation factor modelled for chalk

Authors	Katika, K. & Fabricius, I. L.
Submitted	3rd International Workshop on Rock Physics, Perth, Australia, 13–17 April, 2015

Advanced waterflooding experiments of reservoir rocks are performed on laboratory scale, but the mechanisms that describe the effects of water injection on the rock minerals are poorly understood. The presence of oil and water in the pore space, different ions present in the injected water that contact the pore walls, possible changes in the fluid wetting the surface of the grains and high stress applied on the minerals, comprise the complex system of waterflooding. The changes of the petrophysical and mechanical properties of the rocks affected from waterflooding are the main topic of research in the present study.

DTU Civil Engineering
Technical University of Denmark

Brovej, Bygning 118

www.byg.dtu.dk

ISBN 9788778774415
ISSN 1601-2917